[redacted]

Stem cell migration in the degenerating retina

Martina Pesaresi

TESI DOCTORAL UPF 2019

DIRECTOR DE LA TESI

Dr. Maria Pia Cosma

DEPARTAMENT

Gene Regulation, Stem Cells and Cancer

Centre for Genomic Regulation Barcelona

..Per aspera, ad astra..

ABSTRACT

Retinopathies are a heterogeneous group of conditions that inevitably lead to vision incapacitation and blindness. Currently, they are incurable. Cell therapy has been proposed as a potential solution, but further development and optimization are required. In particular, this study addresses the problem of inadequate migration and integration of transplanted cells into the host tissue. In fact, the majority of the cells transplanted in the eye are unable to reach the injury site, where they are most needed. [redacted].

After identifying the chemokines that are most upregulated during retinal degeneration, [redacted]

The strategy explored in this study provides a way to generate *ad hoc* engineered stem cells with an increased responsiveness to retina-specific signals. Ultimately, our findings could be integrated with alternative optimization strategies to make stem cell therapy in the eye a feasible and realistic option for the treatment of retinopathies, and for the achievement of visual restoration.

RESUMEN DE LA TESIS

Las retinopatías representan un grupo heterogéneo de enfermedades que causan, de forma inevitable, discapacidad visual y ceguera. En la actualidad no se dispone de una cura para estas enfermedades para las que la terapia celular podría ser una solución válida, en el caso de que ésta pudiera ser mejorada y optimizada.

El presente estudio enfrenta el problema de la escasa e inadecuada migración de las células trasplantadas en el tejido diana. De hecho, la mayoría de las células trasplantadas en el globo ocular no consiguen llegar allí donde se las requiere; donde se encuentra la lesión. [redacted]

Después de identificar las quimiocinas más expresadas durante la degeneración de la retina, [redacted]

La estrategia desarrollada en este estudio proporciona una forma de generar células madre con una mayor capacidad de respuesta a

señales específicas de la retina. Tanto es así, que los hallazgos que en él se detallan podrían integrarse con otras estrategias de optimización, de forma que la terapia con células madre sea una opción factible y realista para el tratamiento de retinopatías.

RESUM DE LA TESI

Les retinopaties són un grup heterogeni de condicions que provoquen, de manera inevitable, la incapacitació visual i la ceguera, i és que, malauradament, a dia d'avui no se'n disposa d'una cura. La teràpia cel·lular sorgeix com una solució potencial a aquestes malalties, tot i que encara manca un llarg camí per recórrer.

Concretament, aquest estudi es centrarà en el problema de la migració inadequada de les cèl·lules mare dins del teixit diana, ja que la majoria de cèl·lules trasplantades dins del globus ocular no arriben a la zona lesionada, que és on són necessàries. [redacted]

Una vegada definides les quimiocines més expressades durant la degeneració del teixit retínic, [redacted]

Així doncs, l'estratègia exposada en aquesta tesi proporciona una nova forma de generar cèl·lules mare amb una major capacitat de resposta a senyals específiques de la retina.

Finalment, cal tenir en compte que els resultats obtinguts en el decurs del desenvolupament d'aquest treball podrien arribar a integrar-se amb altres estratègies d'optimització per tal de fer de la teràpia cel·lular al globus ocular una opció factible i realista per al tractament de les diferents retinopaties i, fins i tot, per tal d'assolir objectius tan importants com la restauració visual.

PREFACE

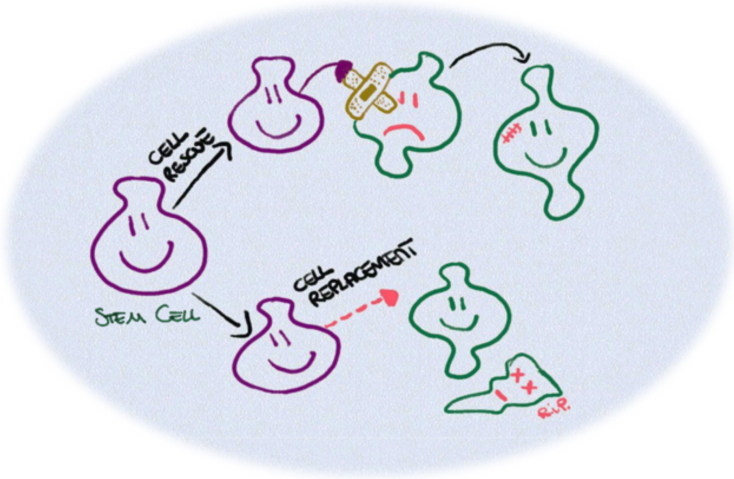

A simplified view of stem cell therapy

Over 250 million people in the world suffer from visual disabilities and blindness. Indeed, it is estimated that every five seconds one person out of five goes blind. In most cases, this is due to conditions that involve damage and/or degeneration of the retina, i.e. the tissue of our body that responds to external light.

In contrast to most invertebrates, mammals cannot regenerate diseased retinae. For this reason, the scientific community is trying to find an alternative solution. Among the various proposals, stem cell therapy stands out for the promising outcomes of both pre-clinical and clinical studies.

Stem cell therapy is based on the injection of stem cells directly into the eye. There, they can help either by providing dying retinal cells with everything they need to survive (cell rescue), or by becoming functional retinal cell types themselves (cell replacement).

Retinal cells at the injury site "communicate" their location through the secretion of soluble signals, called chemokines. In order to pick up these signals, [redacted] Nonetheless, this rarely happens. As a result, only a small percentage of transplanted cells reaches the site of damage, where they are most needed.

Here, [redacted] Transplanted stem cells that reach the injury site slowly start converting into retinal-like cells, as revealed by the fact that they start producing a protein exclusively found in cells with a neuronal phenotype.

Hopefully, our results will contribute to the optimization of stem cell therapies approaches, helping the millions of people that suffer from visual disabilities and blindness as a result of retinal disease and degeneration.

TABLE OF CONTENTS

INTRODUCTION

CHAPTER 1: Retina architecture and retinopathies

1.1 Retina structure and architecture

The retina is the light-sensitive tissue of the body. It lines the inner surface of the back of the eye, and it mediates the first step in the process of vision: it converts light into signals that can be received and interpreted by highly-specialized centers in the brain. Both its anatomy and physiology have been comprehensively characterized. Developmentally, the retina is originated from outgrowths of the embryonic brain; this makes it the most easily accessed area of the central nervous system (CNS) (*1*). Interestingly, all retinal cell types are derived from a common retinal progenitor cell (RPC) population (*2, 3*).

Architecturally, the retina is organized into three main layers (Fig. 1), namely: (1) the ganglion cell layer (GCL); (2) the inner nuclear layer (INL); (3) the outer nuclear layer (ONL) (*4*). Adjacent cells within the same layer are linked through gap junctions, whereas cells from different layers are connected through chemical synapses (*5*).

Ganglion cells represent around 2% of the total retinal neurons, and they are the first specialized retinal cell type that arise during embryonic development.

The INL contains horizontal, bipolar and amacrine cells, which are collectively referred to as interneurons. These are morphologically and functionally distinct neurons. Additionally, the INL contains the cell body of the Müller glia cells (MGCs).
MGCs are the main glial cell type of the retina, where they fulfil typical functions of glia in the CNS. In particular, they are involved in the maintenance of retinal structure, architecture and homeostasis (*6*-*8*); they also actively participate in the regulation of neurotransmitter recycling (*9*).

Finally, the ONL contains the rod and cones photoreceptors, which, together, constitutes about 70 % of the total retinal population. Rods are responsible for black-and-white, dim-light vision; they are extremely sensitive and can detect even a single photon (*10*). Cones, instead, respond to bright light and generate high-acuity color vision. The kinetics of their response are considerably faster than those of rods photoreceptors; however, on average, cones are 100 times less sensitive than rods. While rods are diffusely distributed throughout the retina, cones are spatially restricted to a limited area of the central retina, known as the macula. Within the macula, there is a small, pit-like structure called fovea, which exclusively contains cone photoreceptors. This makes it the point in the retina responsible for maximum visual acuity and color vision.

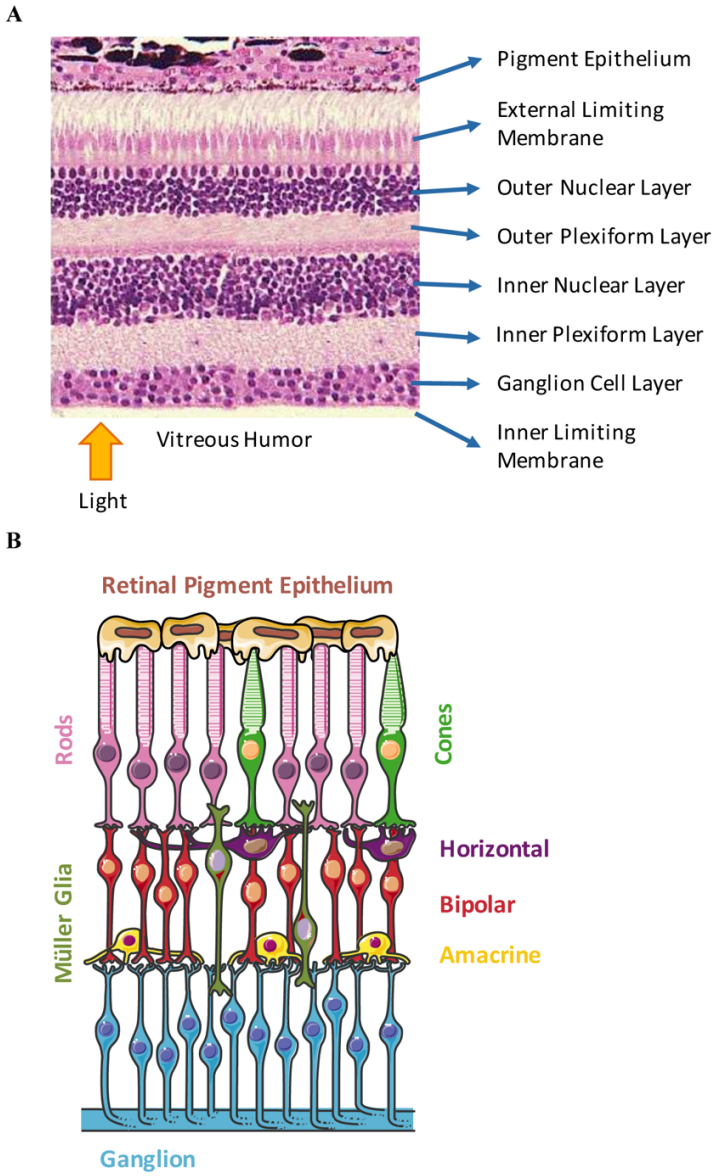

Fig. 1

Fig. 1 - Mammalian retinal structure. (A) Hematoxylin and eosin staining of retinal sections showing the different retinal cell layers. **(B)** Schematic representation of the major retinal cell types and layers. The outer nuclear layer contains rods and cones photoreceptors, and it's lined by the retinal pigment epithelium. Interneurons (i.e., horizontal, bipolar and amacrine cells) and the cell bodies of the MGCs are located in the inner nuclear layer, whereas ganglion cells are found in the homonymous layer.

Light coming from the external environment passes through all retinal layers and it interacts with photoreceptors in the ONL. This interaction induces changes in the membrane potential of photoreceptor cells. Such changes are translated into alteration of neurotransmitter release at synapses. Rods and cones photoreceptors make synapse with rods cones and bipolar cells respectively at the level of the outer plexiform layer. The signals relayed by photoreceptors to bipolar neurons is modulated by horizontal cells. Bipolar cells then connect with amacrine and ganglion neurons at the level of the inner plexiform layer. While amacrine neurons primarily integrate and modulate the signals received by ganglion cells, ganglions project their axons to higher visual centers of the brain through the optic nerve.

1.2 Retinopathies and retina degeneration

Degenerative retinal diseases represent a heterogeneous group of conditions for which no effective therapy is currently available. They inevitably lead to the development of visual disabilities and, in most cases, blindness. Indeed, one in five people in the world are estimated to go blind every five seconds (Fig. 2).

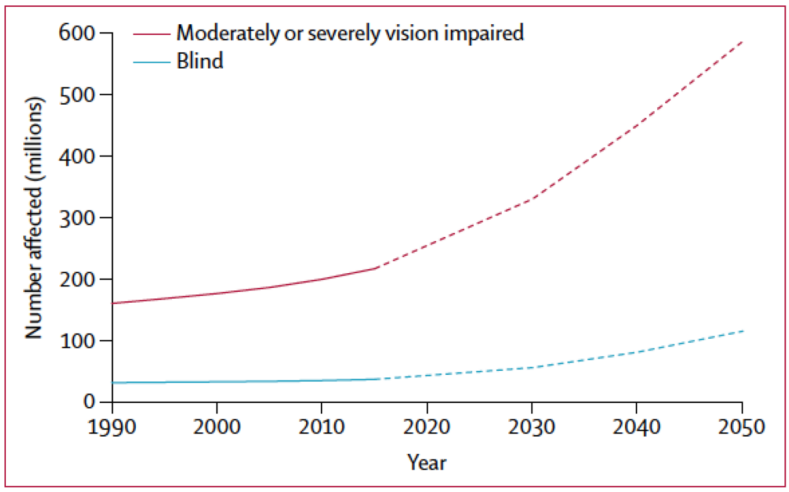

Fig. 2

Fig. 2 – Global impact of retinopathies (from Bourne et al., 2017) (*11*). Global trends and predictions of numbers of people affected by vision impairment or blindness, 1990-2050.

Among all of the retinopathies, age-related macular degeneration (AMD) stands out as the most frequent cause of blindness in the industrialized world (*12*). It is a progressive chronic disease with a polygenic hereditary component (*13, 14*); however, in addition to genetic predisposition, it can also be favored by environmental factors (e.g. smoking or obesity). AMD is characterized by degeneration of the retinal pigment epithelial (RPE) cells, and the consequential defect in the phagocytosis of the photoreceptor outer segment (*15*). This leads to excessive accumulation of lipofuscin, a toxic lysosomal protein that eventually induces photoreceptor apoptosis.

Build-up of lipofuscin is also responsible for an alternative form of

inherited juvenile macular degeneration named Stargardt disease (STGD). STGD affects approximately 1 in 10'000 individuals worldwide and it is associated with gradual loss of central vision (*16, 17*).

Retinitis Pigmentosa (RP) is another frequent form of debilitating and currently incurable retinal dystrophy. It affects 1 in 4.000 individuals, therefore representing the most common inheritable eye disorder. Indeed, more than 100 causative genetic mutations have already been described and characterized (*18*).
RP involves progressive and severe loss of rods and cones photoreceptors. The first symptoms are usually observed in early adulthood, beginning with nyctalopia (i.e. night blindness), continuing with loss of mid-peripheral vision, and eventually culminating with loss of fine central vision and with blindness (*18, 19*).

Laber congenital amaurosis (LCA) is another condition with an autosomal recessive inheritance; it accounts for approximately 5% of all inherited retinopathies (*20*). LCA induces rapid vision loss at birth, and it's usually accompanied by nystagmus and other neurological and systemic abnormalities, including mental retardation (*21, 22*).

Finally, optic neuropathy is a term used to define a heterogeneous group of conditions associated with optic nerve damage, regardless of the cause. Underlying causes can include traumas, infections,

inflammation, autoimmune disease (e.g. neuromyelitis optica), ischemia or glaucoma. Most optic neuropathies can be managed with surgery, corticosteroids, immunosuppressants and other drugs; however, such solutions do not represent a definitive cure, and their effects are only temporary (*23, 24*).

To summarize, as previously mentioned, most retinopathies are currently incurable. On one side, efforts are being made to gain a more in-depth understanding of their underlying mechanisms. This could prove to be instrumental in our understanding of the molecular events that determine normal and aberrant retinal development. On the other side the possibility of using various interventional and potentially curative strategies is being explored. These include gene therapy (especially for monogenetic hereditary diseases), drug cocktails and stem-cell transplants.

1.3 Rodent models of retina degeneration

Numerous rodent models of retina degeneration have been characterized and are currently available. We have decided to proceed in parallel with two of them. On the one hand, we have a pharmacological model of N-methyl-D-aspartate (NMDA)-induced excitotoxicity; on the other hand, we have a genetic model of RP.

NMDA is an amino acid derivative that is remarkably similar to glutamate, the main excitatory neurotransmitter of CNS. Through the

activation of glutamate receptors, intra-ocular administration of NMDA can induce intra-cellular accumulation of calcium. Excessive intra-cellular accumulation of calcium activates a series of neurotoxic cascades. As a result, 30% to 80% of the ganglion and amacrine neurons are lost, in a dose-dependent manner (*25-28*).

The *rd10* mouse model of autosomal recessive RP is characterized by a missense point mutation in the exon 13 of the *Phosphodiesterase 6b* (*Pde6b*) gene (*29, 30*). The *Pde6b* gene is located on chromosome 5 and codes for a peripheral membrane cGMP phosphodiesterase enzyme involved in the phototransduction cascade. As a consequence of their *Pde6b* mutation, homozygous *rd10* animals progressively lose their rods and cones photoreceptors, starting at post-natal day 16 (P16). The peak of retinal inflammation and photoreceptor loss occurs at post-natal day 18 (P18) (*29, 31*). No normal ERG responses can be ever recorded for these mice. However, rod and cone a- and b-waves can be measured at P18; they steadily decline, becoming undetectable at two months of age (*30*).
Compared to the widely used *rd1* model of RP, the *rd10* one is characterized by a later onset and a milder degeneration; therefore, it might provide a better experimental model for the investigation and the development of pharmacological intervention and cell therapy (*29*).

CHAPTER 2: Regenerative medicine

2.1 Tissue regeneration

The term regeneration describes a process that is initiated following injury with the final goal of re-establishing (at least partially) tissue structure and function. Regenerative capacities are not conserved throughout the animal kingdom. As a consequence, some organisms can successfully regenerate entire parts of their bodies, while others can suffer permanent damage following even a mild injury.

During evolution, two main regenerative mechanisms have been selected, namely morphologic and epimorphic (*32, 33*). On the one hand, morphallatic regeneration involves recruitment of stem cells to the damage site; here, stem cells can differentiate into tissue-specific cell types, without passing through a proliferative stage. On the other hand, epimorphic regeneration is based on proliferation of either pre-existing stem/progenitor cells (e.g. planaria) or resident tissue cells (e.g. salamanders). In the case of resident cells, a previous dedifferentiation step is required.

Amphibians, for instance, can replace not only damaged organs, but also entire limbs and tails (*34*). Their remarkable regenerative potential depends on the formation of a specialized structure termed blastema, which involves dedifferentiation of cells located in the proximity of the injury site. “Neoblasts” pass through a proliferative

phase and consequently re-differentiate into tissue cells. This process can regenerate almost the entire body size of the organism(*35*).
Outstanding regenerative potential is also present in animals from other phyla, including Platyhelminthes (e.g. planarians) and Chordates (such as ascidians and zebrafish). As an example, an entire planaria can be formed starting from a tissue fragment that is only $1/279^{th}$ of the original body size. Zebrafish also possess good regenerative capacities. For instance, they can completely regenerate their heart following amputation of up to 20% of the ventricle (*36, 37*).

Nonetheless, in contrast to most cold-blooded vertebrates, mammals have very limited regenerative capacity when it comes to repairing tissues following injury and/or disease (Fig. 3). Years of intense investigations and debates have led to the hypothesis that it is the absence of cell dedifferentiation that underlies this fundamental incapability of repairing tissue damage in mammals. Schwann cells represent a remarkable exception as, when nerve damage occurs, they can dedifferentiate, re-enter the cell cycle and begin to express genes of immature precursor cells (*38*). However, this does not happen following injury in most other organs, including the liver, which undergoes “compensatory regeneration” instead. This means that, in order to replace lost cells and restore physiological function, hepatocytes closed to the injured site re-enter the cell cycle without prior de-differentiation.

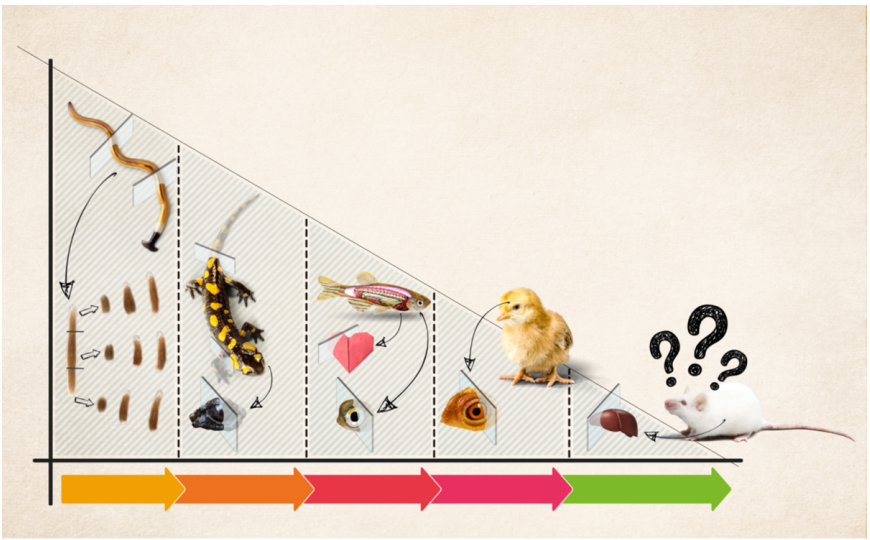

Fig. 3

Fig. 3 – Spectrum of regenerative potential across the animal kingdom (from Pesaresi et al., 2018) (*39*). Platyhelminthes (e.g. planarians) are found on the left-end of the regeneration spectrum, as they are characterized by outstanding regenerative capacities. Amphibians also possess remarkable regenerative capacities; newts, for instance, can fully regenerate their lenses following complete lentectomy (*40*). Regenerative potential is also present in animals from other phyla, including Chordates such as ascidians and zebrafish, which also can completely regenerate damaged retinal tissue (*41*). Potential for retinal regeneration is also maintained in birds, even if only partially. In fact, the avian retina can be efficiently regenerated in the early postnatal period; this capacity, however, is lost as the animal ages (*42*). Mammals are found on the right- (and lower-) end of the spectrum. In fact, the liver is the only mammalian organ that can be endogenously repaired following injury, regaining sufficient function to lead a normal life. Most of the other organs, instead, are endowed with very limited regenerative capacity.

It is however important to highlight how an increasing number of reports are now showing that some mammalian cell types can be induced to dedifferentiate upon stimulation with very specific signals. Such investigations are opening up new and provocative

questions regarding the potential applicability of these methods for the enhancement of endogenous regeneration and the development of regenerative medicine approaches.

2.2 Regenerative medicine

The term regenerative medicine describes a heterogeneous group of approaches and techniques finalized at the re-establishment of tissue homeostasis and functionality following injury. Such approaches generally belong to one of two categories: either stimulation of the body's endogenous regenerative capabilities, or cell therapy.
The focus of this Thesis is on the development and the optimization of stem cell therapy approaches. Therefore, alternatives based on stimulation of endogenous regeneration will only be briefly discussed.

2.2.1 Endogenous regeneration in mammals

Mammalians tissues contain a reservoir of adult stem cells (ASCs) that contribute to the maintenance of tissue homeostasis (*43*). ASCs are located within specialized tissues niches, where they are responsible for the constitutive and physiological turnover of mammalian organs (*44-47*).
The exact kinetics and mechanisms of adult tissue self-renewal have not been thoroughly elucidated yet. However, it is becoming increasingly clearer that turnover rates vary enormously depending

on the organ (*48*). For instance, the intestinal epithelium is completely replaced in less than a week, whereas the heart can take up to several decades (*49, 50*).

ASCs could also potentially become active as a response to tissue damage and inflammation (*47*). Indeed, if exposed to the appropriate stimuli, they can exit quiescence, proliferate and replace lost or deteriorated cells to maintain organ integrity (*51*).
Nonetheless, the regenerative potential of ASCs is not unlimited, and, generally speaking, is characterized by a prominent age-dependent decline. This means that ASCs often are unable to adequately repair severe injuries, such as myocardial infraction and cerebral ischemia; organ integrity is irremediably compromised.
This is why a lot of effort is being put into designing strategies that would promote endogenous regenerative capacities. Possible approaches include activation of resident stem cells, or reprogramming of other healthy resident cells *in vivo* (*52-56*).

These types of strategies offer multiple advantages. For instance, the cells that would eventually mediate regeneration are already physically located in the proximity of the injury, where they are needed. In this way, migration and integration difficulties are greatly reduced, if not eliminated. Contemporarily, differentiation into tissue-specific cell types is promoted by the exposure to the appropriate local microenvironment. The problem of immune rejection is also avoided, as newly generated cells will be autologous by definition. Furthermore, the risk of tumorigenesis is lowered (*57,*

58). Importantly, promoting the body's self-repair capabilities would also remove from the equation the need of thoroughly assessing cells' integrity and phenotype prior to transplantation.

2.2.2 Endogenous regeneration of the retina

Retinal tissue can be regenerated via one of two main strategies. Resident stem cells present in the ciliary body (CB) or in the ciliary marginal zone (CMZ) can exit quiescence and become active, proliferating and replacing lost retinal cells. Alternatively, resident retinal cells can undergo dedifferentiation and generate retinal progenitor cells (RPCs). RPCs are multipotent progenitors that first proliferate and then differentiate into all retinal cell types (*59*).
In particular, there are two main cell types that can be converted into RPCs: MGCs and cells of the retinal pigmented epithelium (RPECs). RPECs are the main players in regenerating the amphibian retina, whereas MGCs represent the main source of retinal regeneration in zebrafish (*60-62*) and chicken (*42, 63, 64*).

Even in mammals, MGCs can re-enter the cell cycle and contribute to neuronal regeneration following pharmacological damage of either ganglion or photoreceptor cells (*65-70*). Importantly, activated MGCs tend to differentiate into the cell type that has been damaged (*66, 71, 72*). However, the frequency of such events is extremely low and the regenerative potential of mammalian MGCs is very limited. As a consequence, proliferative MGCs are unable to fully rescue retinal functionality (*73*).

Over the past 10-15 years, some of the signaling pathways and the molecular mechanism involved in endogenous retinal regeneration have been characterized. For instance, MGCs can be stimulated by overexpression of *Ascl1*, a transcription factor essential during retinal development (*74, 75*). Remarkably, MGC reprogramming ability can be further increased when *Ascl1* over-expression is combined with inhibition of a histone deacetylase, which results in a more open chromatin state that favors accessibility at key gene loci (*76*). Pharmacological perturbation of Wnt/β-catenin, EGF, FGF, Cxcr4-Sdf1 and insulin pathways can also stimulate the neural regenerative potential of mammalian MGCs (*65, 67-69, 77-80*).

CHAPTER 3: Stem cell therapy

3.1 Stem cell therapy

As the name strongly suggests, stem cell therapy approaches are based on the transplantation of either stem or progenitor cells (Fig. 4).

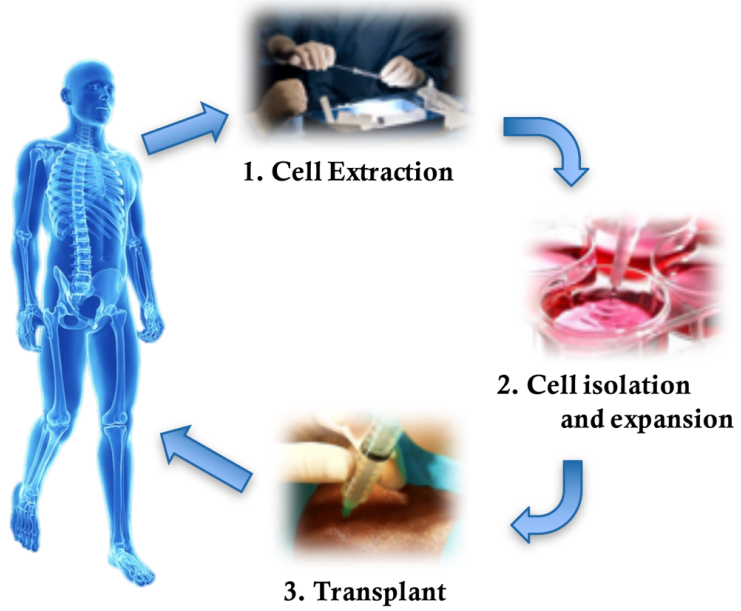

Fig. 4

Fig. 4 – The three steps of cell therapy approaches. The overall cell therapy procedure involves three distinct steps: (1) cell extraction - cells are extracted from a donor, who, importantly, can be the patient themselves; (2) cell isolation - cells are isolated and, if possible, cultured, expanded and/or differentiated; (3) transplant - finally, cells are transplanted back into the patient, with the aim of restoring tissue functionality.

Therapeutically, stem cells (SCs) can exert beneficial effects in one of two ways (Fig. 5).

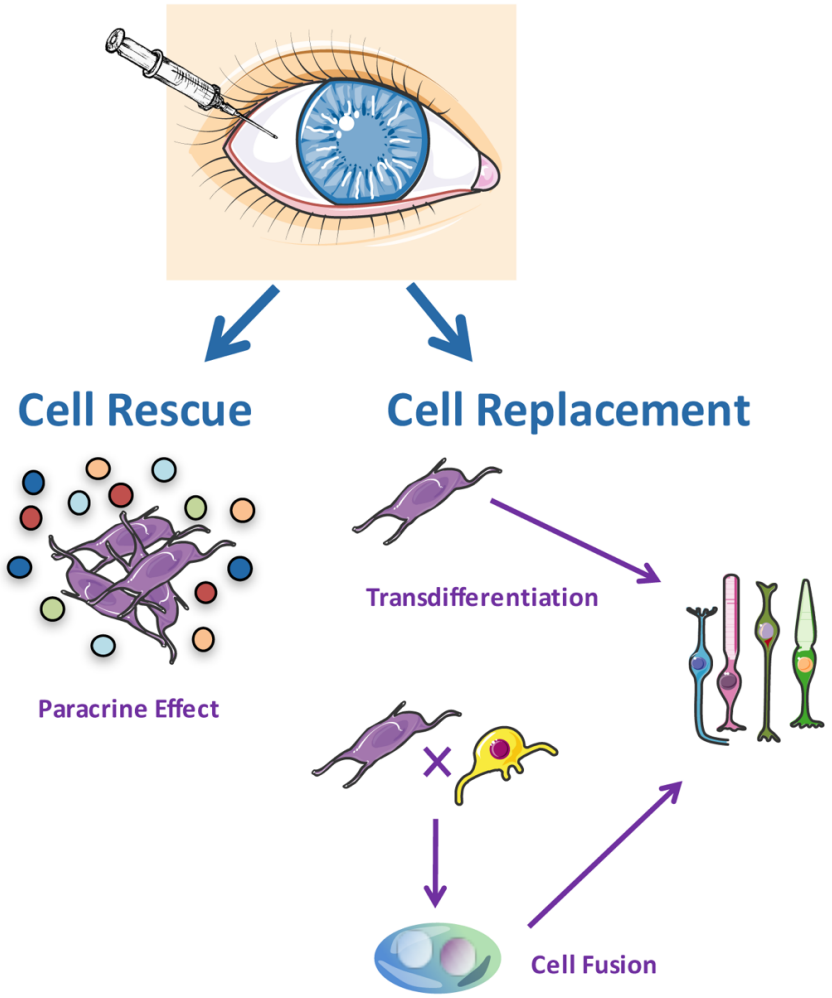

Fig. 5

Fig. 5 – Mechanisms of stem cell therapy beneficial effects. On the one side, stem cells can promote survival and recovery of endogenous cells through the secretion of neurotrophic factors and other biologically active molecules with anti-inflammatory properties (i.e. the paracrine effect). On the other side, they can integrate within the tissue and differentiate themselves into new functioning tissue-specific cell types, thereby replacing lost and/or damaged cells. This can occur via either transdifferentiation or cell fusion-mediated events.

On the one side, they can secrete biologically active molecules in a process that is termed paracrine effect. The paracrine effect of SCs has neuroprotective and anti-inflammatory properties; it strongly promotes cell survival and recovery.
On the other side, SCs can generate new functioning tissue-specific cell types, thereby replacing lost and/or damaged cells. To promote and facilitate this process, SCs can be differentiated towards specific desired progenitor types *in vitro*, prior to transplantation. Importantly, the possibility of culturing and expanding cells *in vitro* facilitates the obtainment of abundant starting material; this, in turn, significantly increases the probability of adequately replacing lost tissue.

However, several issues remain to be satisfactorily addressed. For instance, cell therapy can raise important concerns with respect to the risk of tumorigenesis; indeed, most protocols and procedures for the generation of clinical-grade cells remain to be established and standardized (*81*). Furthermore, beneficial outcomes are generally dampened by poor migration and poor functional integration of transplanted cells within the host tissue.

For these reasons, currently, cell therapy is routinely used only for bone marrow replacement. Significant advances are required to establish its reliability and therapeutic value in other tissues and organs.

3.2 The eye as a target for cell therapy approaches

The eye represents an exceptionally good target for the first generation of CNS cell therapy approaches.
Firstly, both the anatomy and the physiology of the eye and of the retina have been extensively characterized. Secondly, surgical techniques are already well established and routinely performed in clinics, with excellent safety records (*82*). Thirdly, patients and transplant functionality can be monitored continuously and with minimal risk thanks to the availability of numerous non-invasive and high-resolution ocular imaging techniques; these techniques include optical coherence tomography (OCT), fluorescein angiography (FA) and adaptive optics scanning laser ophthalmoscopy (AOSLO) (*83-87*). Fourthly, since the eye is a small and encapsulated organ, a relatively small number of viable transplanted cells would most likely be sufficient to support visual restoration (*88*).
Additionally, most retinopathies initially affect a single cell type, meaning that therapy could be focused on the replacement of one specific cell group. Finally, under non-disease circumstances, the subretinal space is an immunoprivileged site; this means that cell grafts are significantly less likely to be rejected (*89, 90*).

For all of these reasons, stem cell therapy represents an attractive and promising possibility for the treatment of retinal diseases. Indeed, plenty of pre-clinical studies have extensively shown the beneficial effects that stem cell-based therapies can have in rodent models of retinal injury and degeneration (Table 1). Moreover, we are now starting to gather the results coming from over a decade of clinical

trials, performed using a variety of cell sources with patients affected by a wide range of diseases. It is important to stress that most trials have not reached pre-established endpoint. However, the available preliminary results are encouraging.

Cell type	**Disease**	**Route**	**Animal Model**	**Reference**
MSCs	Retinal degeneration	S	Rat (RCS)	(*91, 92*) (*93*)
			Rat (Light-damage)	(*94*)
	RP	S	Mouse (Rhodopsin KO)	(*95*)
	Glaucoma	I	Rat (Laser-induced ocular hypertensive glaucoma)	(*96*)
			Rat (Ligation of episcelar veins)	(*97*)
	Trauma	I	Rat (Optic Nerve Transection)	(*98, 99*)
BMDCs	Retinal degeneration	S	Rat (RCS)	(*100*)
		I	Mouse ($Pde6b^{Rd1}$ and $Pde6b^{Rd10}$)	(*101*)
	RP	S	Mouse ($Pde6b^{Rd10}$)	(*102*)
		I	Mouse (NMDA-induced RGC degeneration)	(*71*)
	Trauma	I	Mice (Laser injury)	(*103*)
	Retinal vasculopathy	I	Mice (Acute retinal ischemia-reperfusion injury)	(*104*)
ESC or iPSC-derived RPECs	Retinal degeneration	S	RCS Rat	(*105-107*) (*108*)
	STGD	S	Elov14 Mouse	(*105*)
RPECs	Retinal degeneration	S	RCS rat	(*109*)

NPCs	Retinal degeneration	S	RCS rat	(*110, 111*) (*112*)
		I	Mouse (*mnd* mouse – lysosomal storage disease with retinal and CNS degeneration)	(*113*)
	RP		Mouse ($Pde6b^{Rd1}$ and $Pde6b^{Rd10}$)	(*114*)
	Trauma		Rat (Mechanical injury)	(*115*)
	Ischemia		Rat (Damaged by acute ocular hypertension)	(*116*)
RPCs	RP	S	Mice (Rhodopsin KO)	(*117*)
			Rat (Mutations in the rhodopsin gene)	(*118*)
PRPs	RP	S	Mouse (Rhodopsin KO)	(*81*)
	Congenital stationary night blindness		Mouse ($Gnat1^{-/-}$, lacking rod function)	(*119*)
hMGC-derived RGCs	RGC degeneration	I	Rat (NMDA-induced RGC degeneration)	(*120*)

Table 1 (adapted from Sottile et al., 2019) (*121*) - Comprehensive list of stem cell-based studies in rodent models of retinal degeneration and disease (MSC = mesenchymal stem cells; BMDCs = bone marrow-derived cells; ESCs = embryonic stem cells; iPSCs = induced pluripotent stem cells; RPECs = retinal pigmented epithelium cells; NPCs = neural progenitor cells; RPCs = retinal progenitor cells; PRPs = photoreceptor precursors; hMGCs = human Müller glia cells; RGCs = retinal ganglion cells; S = subretinal injection; I = intravitreal injection)

3.2.1 The immune privilege of the eye

Broadly, a site is defined as immunoprivileged if foreign tissue grafts that would normally be rapidly rejected can survive there for extensive periods of time.
The immune privilege of the eye makes perfect sense from an evolutionary point of view. In fact, in the process of eliminating foreign pathogens, antigen-specific immune responses often cause the destruction of some adjacent tissue, in a process that is often called bystander injury. Bystander injury would not cause irreparable damage to bigger organs (such as the heart, or the liver), but it would surely have devastating effects in the eye, especially if spatially located in the proximity of the fovea (which, as already discussed, is responsible for central vision).

The immune privilege of the eye is achieved thanks to both anatomic and functional factors. Anatomic factors include, for instance, the absence of lymphatic drainage and, most importantly, the presence of a blood-retinal barrier. This is formed by tight junctions between RPECs (which protect the outer retina) and retinal vascular endothelial cells (which protect the inner retina). Partial physical isolation is further reinforced by the establishment of an intraocular immunosuppressive microenvironment (*122*), in which: (1) antigen-presenting cells are tolerogenic; (2) T-cell activation is inhibited by direct cell-to-cell contact and cytokine secretion (*123*); (3) $CD8^+/CD4^+$ cytotoxic T lymphocytes are converted into regulatory T cells (*124, 125*); (4) numerous soluble immunosuppressive factors

are constitutively secreted. Furthermore, activity of the complement system is tightly regulated. More specifically, the complement system is chronically activated at low levels as a preventive protective measure against pathogens and infections.
At the same time, the harmful effects of inadvertent and/or excessive complement activation are prevented by various soluble and membrane-bound regulatory molecules (*126, 127*). In this way, the risk of functional tissue destruction is minimized (*126, 127*). Additionally, corneal epithelial cells and endothelial cells express no class II MHC antigens, and only very low levels of MHC class I molecules (*128*) This means that they will be "invisible" to surveilling immune cells. Such "immunologic ignorance" of the tissue is at the very heart of the success of corneal transplantation.

3.2 Stem cell sources

Stem cells are defined by three fundamental properties. Firstly, they are capable of self-renewal and can proliferate indefinitely. Secondly, they exist in an undifferentiated state, with no specific cell fate defined. Thirdly, they can differentiate towards various types of cells and tissues. In particular, pluripotent SCs can give rise to all cell types of the body (endoderm, ectoderm, mesoderm), with the exception of those forming extra-embryonic tissues (e.g. the placenta) (*129, 130*). Multipotent SCs, instead, can only differentiate into a limited number of cell types that will generate certain tissues.

Both pluripotent and multipotent SCs represent potential sources for cell therapy in the eye (Fig. 6).

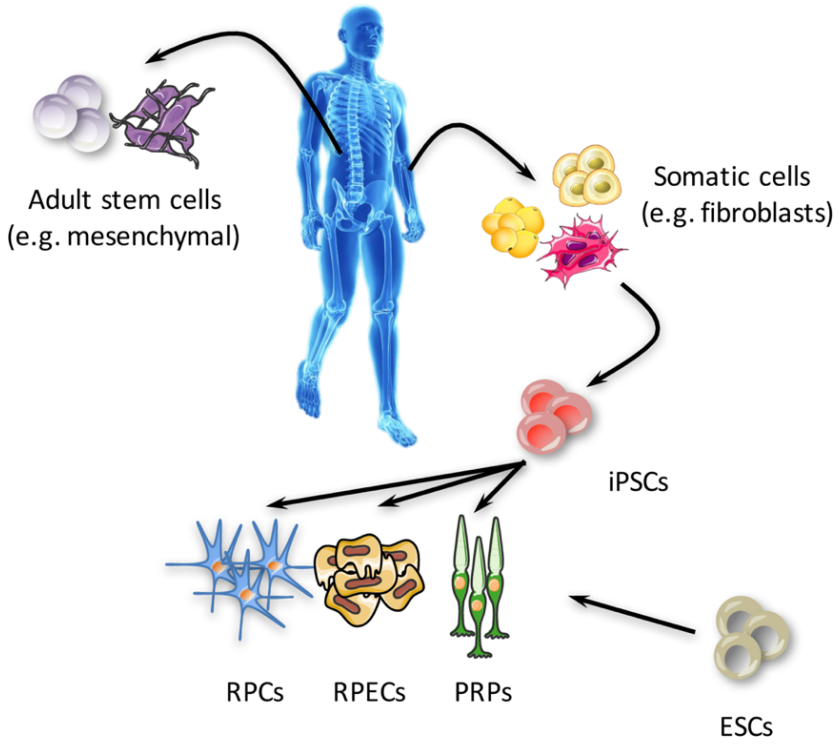

Fig. 6

Fig. 6 – Potential sources for cell therapy in the eye. Cell therapy approaches can be developed starting from either adult stem cells (e.g. HSPCs, MSCs) or somatic cells that have been converted to iPSCs. Alternatively, pluripotent stem cells can be obtained from the early embryo (i.e., ESCs). ESCs/iPSCs can then be differentiated prior to transplantation (e.g. in retinal progenitor cells – RPCs; retinal pigmented epithelium cells – RPECs; or photoreceptor precursors – PRPs).

3.2.1 Pluripotent stem cells

Embryonic stem cells (ESCs) are pluripotent cells that can give rise to entire new organisms (*131*). They were isolated for first time in the early 1980s, when the groups of Martin Evans and Gail R. Martin independently derived them from the inner cells mass (ICM) of the early blastocyst.
Induced pluripotent stem cells (iPSCs), instead, are a type of pluripotent cells that can be derived from accessible adult tissues. They were generated for the first time in 2006, when Shinya Yamanaka transduced mouse fibroblasts with a set of four defined transcription factors, namely Oct4, Sox2, Klf4 and c-Myc (or OSKM) (*132, 133*).

Due to their proliferative activity and their differentiation potential, ESCs and iPSCs potentially represent the single cell source that could be used to regenerate multiple tissues and organs. Indeed, countless protocols are available to efficiently differentiate them towards very specific lineages of choice (*133-135*).
Transplantation of iPSC-derived cells has already been proven beneficial in rodent models of sickle cell anaemia (*136*), Parkinson's disease (*137*), diabetes (*138*), and spinal cord injury (*139*). In the attempt of treating retinopathies, mouse and human pluripotent SCs have been used as a starting point to generate not only neural precursors cells (NPCs) (*140*), but also RPCs (*141*), RPECs and photoreceptor precursors (PRPs) (*142*).

SC-derived NPCs are able to successfully integrate within the recipient retina. Moreover, they can moderately delay photoreceptor degeneration thanks to their phagocytic activity (*112, 114, 143, 144*). However, they are fundamentally incapable of differentiating into mature retinal cell types (*115, 116, 145*).
RPCs, RPECs and PRPs, instead, are highly efficient in generating mature ganglion neurons and photoreceptors. Indeed, SC-derived photoreceptor precursors produce normal calcium oscillations, and, when transplanted into animal models of ONL degeneration, they can rescue visual function to some extent (*81, 146-148*). However, their functional integration into the retinal neural circuit remains worryingly low (*107, 113, 142, 149, 150*).

The use of ESCs and iPSCs for clinical purposes is associated with a number of issues. For instance, the cost of derivation and differentiation protocols is considerably elevated. More disturbingly, transplantation comes with an intrinsic high risk of teratoma and malignant tumor formation (*81, 151*). As an example, ESCs-derived NPCs have been reported to generate teratomas in 50% of treated animals in the long term (*152*). However, the tumorigenic side-effects are strongly believed to be mediated by residual pluripotent cells; if that was really the case, then they could be eliminated through the establishment of detailed, standardized differentiation protocols and strict quality and purity control procedures. In other words, terminally differentiated ESC/iPSC-derived cells do not seem to pose a threat with respect to tumor formation (*81, 108*). Accordingly, no tumors formation was observed in a cohort of 45 immunodeficient

mice (lacking both mature T and B cells) transplanted with ESC-derived RPE cells (*105*).

hESC derived RPE cells have also been transplanted in human patients with Stargardt or AMD in a phase I clinical trial. The trial met its safety endpoint, with no adverse effects being reported (*153*). Actually, only one eye showed worsened best-corrected visual acuity, whereas the majority of patients benefited from a modest, but sustained, improvement in visual acuity (*154*). Transplanted cells appeared to engraft at the boundaries of areas where endogenous RPECs and photoreceptors had undergone atrophy (*154*).

Interestingly, in addition to SC-derived PRPs, sheets of fetal and cadaveric photoreceptors have also been transplanted in human patients. Such grafts were reported to be safe and to last for extended periods of time without eliciting any immune reaction, even though patients were not immunosuppressed (*155, 156*). This is consistent with the fact that the immunogenicity of photoreceptors is lower than that of RPECs (*157-159*). However, transplanted photoreceptors were unable to rescue visual function.

3.2.1.1 ESCs or iPSCs?

iPSCs generation does not involve destruction of pre-implantation stage embryos, thereby eliminating much of the ethical and moral controversy associated with the use of ESCs. Additionally, their availability is not limited, and they can be used to create autologous,

patient-matched cells that would theoretically not be rejected by the recipient immune system (*133, 160*). For instance, when subretinally transplanted, iPSC-derived RPECs from MHC-matched donor and recipient can survive without the need for immunosuppression (*161*). Nonetheless, immune response is rapidly elicited by MHC-mismatched grafts. This implies that there still are considerable concerns regarding the potential immunogenicity of iPSCs (*162-164*).

The use of iPSCs also faces challenges in the context of genetic diseases. In fact, iPSCs derived from the patients will still harbor the disease-causing mutation; genetic correction would thus be required prior to transplantation.
Moreover, iPSCs have been traditionally associated with safety concerns deriving from the use of viruses to express the OSKM reprogramming factors in somatic cells. In fact, OSKM-carrying viral vectors randomly integrate in the host genome, potentially causing unpredictable mutations. To address this concern, new protocols are being developed; some of them eliminate the need for potentially transforming factors such as *c-Myc* or *Klf4*, while others rely on the use of non-viral vectors (*165-172*). In both cases, the safety of iPSCs is increased.

It is also important to consider that gene expression and DNA methylation profiles of iPSCs can be significantly different from that of their naturally-occurring counterparts (*173*). For instance, hiPSC-derived RPECs show a gene expression profile that significantly

differ from that of human fetal RPE, whereas that of ESC-derived RPECs is much more similar to the endogenous one (*174*).

To sum up, the use of ESC/iPSC for therapeutic transplants has not reached a sufficiently advanced and safe stage yet. Nonetheless, it holds a tremendous potential for the further development of cell replacement strategies. Indeed, various clinical trials have been conducted or are currently underway to investigate the effects of hESC-derived RPE cell transplantation in multiple conditions, including AMD and Stargardt disease (*175*).
Preliminary results are encouraging, as they provide some evidence that hESC-RPEC grafts can survive for several months and have some biological activity. Even though some patients showed signs of hyperproliferation, no excessive inflammatory response or tumorigenic side-effects have been reported to date (*175, 176*).
Special attention should and will be placed in evaluating the long-term risk of tumor formation and immune rejection.

3.2.2 Adult stem cells

As already discussed, ASCs are multipotent cells that can generate subsets of cells belonging to specific lineages. Over the past couple of decades, numerous protocols to isolate and culture ASCs have been defined. This has allowed not only to gain insights into the molecular mechanisms regulating their regenerative capabilities, but also to start exploiting them for the establishment of new therapeutic approaches (*177, 178*).

Retinal progenitor cells (RPCs) are located within the pigmented ciliary epithelium of adult mammals and are intrinsically efficient at differentiating into mature retinal cell types (*119, 179-183*). When transplanted subretinally, they can improve visual behavior not only in mice, but also in human patients with photoreceptor loss (*184-186*).
However, their migratory ability is very poor and harvesting them remains technically challenging. Indeed, for the time being, their availability is extremely limited and associated with considerable ethical concerns, as they can only be isolated from fetal tissue (*187*).

Among all other ASCs, hematopoietic stem and progenitor cells (HSPCs) and mesenchymal stem cells (MSCs) can be regarded as the most promising sources for the further development of stem cell-based therapy in the eye.

3.2.2.1 Hematopoietic Stem and Progenitor Cells

The bone marrow represents an attractive source of ASCs. In fact, it contains HSPCs, which are responsible for the maintenance of the hematopoietic tissue homeostasis and for the generation of both red and white blood cells. HSPCs are used for the treatment of patients with conditions like anemias. Such patients are incapable of producing healthy red blood cells, and are treated through the replacement of their HSPCs with the bone marrow of a healthy donor.

Bone marrow cells are also used for the treatment of some blood cancers, including leukemia. In this case, bone marrow cells are wiped out by chemotherapy, and replaced in order to provide the patient with a functioning immune system.

In the late 1990s, bone marrow-derived cells (BMDCs) were shown to possess a wider plasticity than previously assumed. They were reported to migrate to several organs, where they could generate a variety of different cell types that included myocytes (*188*), cardiomyocytes (*189, 190*), hepatocytes (*191, 192*) and neurons (*193-195*). This could occur via either trans differentiation or cell fusion-mediated events. As a consequence of such observations, the therapeutic potential of HSPCs started to be intensively investigated in other disease contexts, including retinopathies.

Evidence for the beneficial and neuroprotective effects of HSPCs in the context of retinopathies is steadily accumulating, not only in experimental animal models (*92, 101, 196-198*), but also in human patients (*104, 199*). As an example, our group has shown that Wnt-activated HSPCs can ameliorate retina degeneration following NDMA-damage and in the *rd10* mouse model of (*71, 72*). In these cases, the therapeutic outcome was dependent on the fusion of transplanted HSPCs with resident MGCs. Resulting hybrids passed through a proliferative phase and eventually differentiated into ganglions, amacrine cells and photoreceptors, thus participating in the repair of the retinal tissue.

3.2.2.2 Mesenchymal Stem Cells

During development, MSCs are responsible for the generation of adipocytes, chondrocytes and osteocytes. However, under the appropriate environmental stimuli, they display a much broader differentiation potential, generating other cell types that include cardiomyocytes, skeletal muscle cells and even neural cells (*200-202*).

Most adult tissues contain MSC populations. However, MSCs are primarily concentrated in the bone marrow and in the adipose tissue. In the bone marrow, they serve as haematopoietic-supporting stromal cells (*203-205*). Although MSCs constitute a mere 0.001-0.1% of the total bone marrow cell population, they can be rapidly and easily expanded ex-vivo (in contrast to HSPCs). Importantly, this allows for production of MSCs on a clinical scale.

Recently, a set of minimum criteria for cells to be considered MSC has been defined (*206*). In addition to their osteogenic, adipogenic, and chondrogenic differentiation capacity, MSCs have a fibroblastic morphology and spontaneously adhere to plastic substrates. Moreover, they are positive for CD73, CD90 and CD105 expression, but negative for CD34, CD45, CD14, CD11b, CD19, CD79α or HLA-DR.

MSCs mainly exert their beneficial effects through their paracrine activity (Fig. 7).

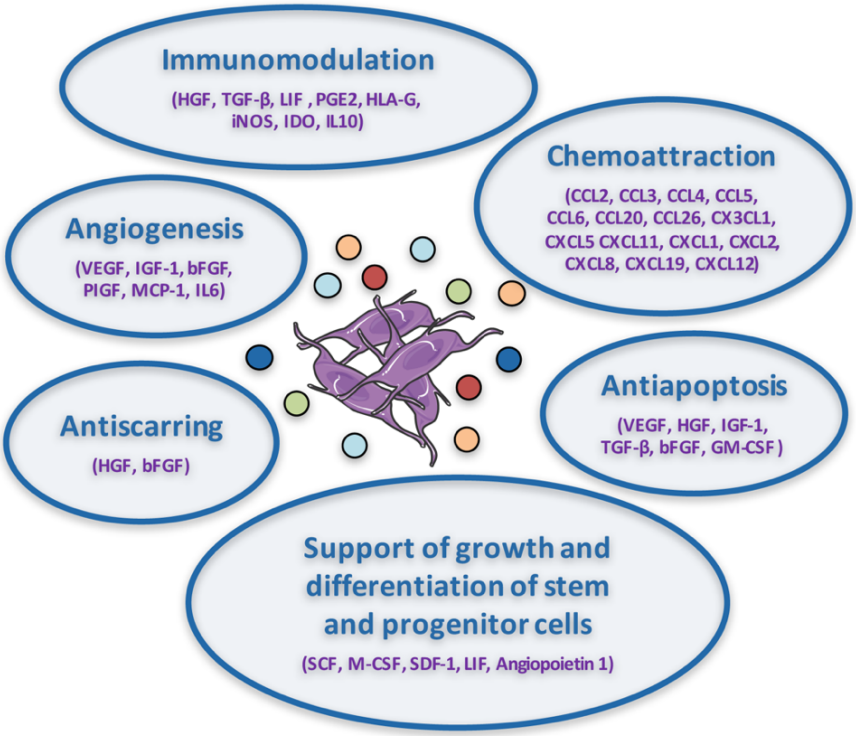

Fig. 7

Fig. 7 – MSC paracrine activity. The paracrine activity of MSCs can be divided into six main actions: (1) immunomodulation; (2) chemoattraction; (3) anti-apoptotic signaling; (4) activation and support of local stem cells; (5) antiscarring and beneficial remodeling of the extracellular matrix; (6) increased angiogenesis to chronically ischemic tissues (*98, 207, 208*). In particular, MSCs suppress apoptosis through secretion of vascular endothelial growth factor (VEGF), hepatocyte growth factor (HGF), insulin-like growth factor 1 (IGF-1), transforming growth factor β (TGF-β), basic fibroblast growth factor (beg), and granulocyte macrophage colony–stimulating factor (GM-CSF). Ischemia-induced scarring is inhibited by HGF and bFGF, while angiogenesis is promoted by VEGF, IGF-1, bFGF, phosphatidylinositol-glycan biosynthesis class F protein (PIGF), monocyte chemoattractant protein 1 (MCP-1), and interleukin 6 (IL-6). They also promote activation of tissue-resident stem and progenitor cells by secreting stem cell factor (SCF), macrophage colony–stimulating factor (M-CSF), stromal cell–derived factor (SDF-1), leukemia inhibitory facto (LIF), and angiopoietin 1. A group of at least 15 chemokines produced by MSCs can elicit leukocyte migration to the injured area. Finally, MSCs mediate their immunomodulatory effects by strongly inducing the M2-alternative polarization of macrophages; this boosts IL-10 production and cytoprotection (*209*). Contemporarily, they inhibit the maturation of antigen-presenting cells and the activity and proliferation of natural killer (NK)

cells and of $CD4^+/CD8^+$ double positive cytotoxic T lymphocytes, while promoting the maturation of T cells towards the regulatory $CD4^+/CD25^+$ phenotype (*210-215*). Such effects are induced through the secretion of factors such as HGF, prostaglandin E2 (PGE2), human leukocyte antigen G5 (HLA-G5), inducible nitric oxide synthase (iNOS), indoleamine-2,3-dioxygenase (IDO), and interleukin 10 (IL-10).

In particular, they secrete a plethora of cytokines and neurotrophic factors that are critical for the repair of injured tissues; these include NGF, BDNF, NT-3, NT4/5, CNTF, GDNF and PDGF (*216-227*). In this way, MSCs can potently stimulate the survival, the proliferation and the self-repair capabilities of endogenous cells, often resulting in the slowdown of disease progression (*95, 100, 228*). It is important to stress that, in contrast to that of MSCs, the secretome of ESCs and iPSCs has not been proven to have any beneficial paracrine effect in the context of retinal disease.

MSCs also have prominent immunomodulatory properties. When exposed to tissue injury and inflammation, they acquire a potent anti-inflammatory, immunosuppressive and protective phenotype.

Furthermore, MSCs have little or no immunogenicity, due to their relatively low expression of the Major Histocompatibility Complex (MHC) class I proteins, and to the absence of MHC class II molecules at the cell surface (*229-231*). Thanks to their almost negligible immunogenicity, MSCs represents very good candidates for the development of not only autologous, but also allogenic therapies (*100, 232*). On the contrary, the immunogenicity of iPSCs appears more complex, and it requires careful study before clinical application (*162, 163*).

3.2.2.2.1 Mesenchymal stem cell sources

Traditionally, MSCs have been derived from the bone marrow (BM-MSCs). BM-MSCs, however, are characterized by a limited growth rate and a quality that is mostly dependent on the age of the donor. Additionally, there are some considerable risks in sample collection. For these reasons, nowadays, there is a growing interest in the use of MSCs derived from alternative sources.

MSCs can be isolated with less invasive methods from full-term umbilical cord blood (UCB) donations. Subretinal injection of UCB-MSC seems to improve visual function in a rat model of retinitis pigmentosa (*91*). However, the success rate of isolation is considerably lower than that of BM-MSCs, and their adipogenic differentiation potential seems to be impaired (*233*).

Adipose tissue-derived MSC (AD-MSCs) probably represent the most attractive alternative to BM-MSCs. In fact, AD-MSCs can be easily collected in high amounts from liposuction procedures. Moreover, compared to BM-MSCs, they display not only higher proliferative rates, but also higher secretion of some neurotrophic factors, including BDNF and VEGF (*233, 234*).
Unfortunately, the therapeutic potential of AD-MSCs remains largely untested in the eye. Nonetheless, their neuroprotective effects have been extensively described in other models of CNS injury and degeneration, including spinal cord injury (*234, 235*) and stroke (*236*).

Recently, dental pulp-derived MSCs (DP-MSCs) are also being investigated. Analogously to the other MSC populations, DP-MSCs do not stand out for their ability to migrate and integrate within the host retina (*99*). However, they secrete more neurotrophic and protective factors than BM-MSC, and they can promote neurite outgrowth with higher efficacy than both BM-MSCs and AD-MSCs (*99, 237*).

3.3 Routes of administration

Stem cells can be delivered via one of three routes: intravitreal, subretinal and systemic.

Systemic administration is based on intravenous infusion of cells. Compared to the other routes, it generally has a significantly lower efficiency, especially in the case of MSCs. This is mostly due to the fact that MSCs are recruited and trapped in the lungs (*238*). Additionally, even if they escaped lung entrapment, their migration into the tissue would be further prevented by the blood-retinal barrier. This could explain why systemically transplanted MSCs fail to reach the retina and to exert neuroprotective effects (*239*). Therefore, intravitreal or subretinal routes are typically preferred, at least in the context of retinal diseases.

Overall, the suitability of each administration route may vary depending on the type and on the extent of tissue damage. Indeed, the

disease type appears to majorly affect the outcome of the therapy. For instance, the success of rod-photoreceptor transplant has been shown to vary across six different models of inherited photoreceptor degeneration and also with disease progression (*240*). As a general rule, intravitreal injection is preferred when ganglions and/or INL cells are damaged, whereas subretinal administration is the standard route in the context of photoreceptor loss.

Intravitreal transplantation represents an attractive choice, as it is technically simple and minimally invasive. It also allows for injection of relatively large volumes. Indeed, numerous studies have shown that intravitreal injection of MSCs is beneficial in various models of glaucoma and retinal dystrophy (*97, 239*). Moreover, integration into the RGC layer and into the INL appears to be favored following intravitreal transplantation rather than in subretinal grafts (*241*).
However, intravitreal injection does not target cells directly into the host tissue; cells have to pass through the vitreous, where they will be exposed to macrophages and other immune cells. Moreover, transforming cells in the vitreous have the potential to induce proliferative vitreoretinopathy and retinal detachment (*242*).

Subretinal transplantation is a much more challenging, demanding and complex procedure. If the integrity of the blood-retinal barrier is compromised during surgery, then the immunoprivilege of the subretinal space is lost, and immunosuppressive therapy becomes necessary. However, when correctly performed, subretinal implants generally provide greater and longer-lasting benefits than their

intravitreal counterparts, especially in the context of photoreceptor degeneration (*93, 243*). Indeed, the subretinal microenvironment can better support and promote the differentiation of precursors cells towards photoreceptors (*150, 241*).

Moreover, subretinal grafts are generally associated with better migration and integration, also owing to the closer proximity of the transplant site to the injured retinal layers. Importantly, this correlates with increased therapeutic effects (*93*). This may be especially relevant from a clinical perspective, as human eyes have a comparatively larger globe and a thicker retina. As a result, transplanted cells would have to cover larger distances and pass through a thicker neuroretina before reaching the ONL. Furthermore, secreted cytokines and neurotrophic factors would probably be excessively diluted.

Finally, it is interesting to comment that cells can be injected not only as suspensions, but also as monolayers supported by scaffolds. Scaffolds could be natural or synthetic, biodegradable or non-biodegradable. Several different types and variations are being studied, and some of them have provided encouraging results *in vivo* (*244-246*). This could be of particular importance for RPE replacement (e.g. in the case of AMD), as, when transplanted as a cell suspensions, RPECs tend to clump and fail to properly attach to the vitreous lamina (*247*). As an alternative, they can be transplanted on supportive scaffolds that closely resemble the native Bruch's membrane, which normally lies between the RPE and the choroidal vessels. Bruch's membrane is involved in the regulation of diffusion

of materials between the retina and choroid; additionally, it supports RPECs on its basal side (*248*). As a proof of principle, confluent RPEC monolayers have been delivered using vitronectin-coated polyester membranes (*244*) and parylene C scaffolds (*249*). In both cases, improved integration and cell function were reported. However, additional studies are still required to combine the best cell type for transplantation with the appropriate scaffold.

3.4 Migration and integration for cell replacement

The advancement of effective stem cell therapy approaches has been limited by inadequate migration and integration rates into the host retina. On average, less than 1% of the transplanted cells are engrafted within the tissue (*92, 182, 250-252*), especially following intravitreal injection (*97, 208*). This can somehow be ascribed to the presence of two physical barriers, on either side of the retinal layers (Fig. 8).

The inner (ILM) and outer (OLM) limiting membranes prevent the migration of intravitreally (*97*) and subretinally transplanted cells respectively. Accordingly, engraftment of transplanted photoreceptor precursors has been reported to significantly improve when the OLM is temporarily disrupted (*253*). Interestingly, if the phenotype of a given disease included physical disruption of the retinal barriers, then integration of transplanted cells would be promoted (*240*).

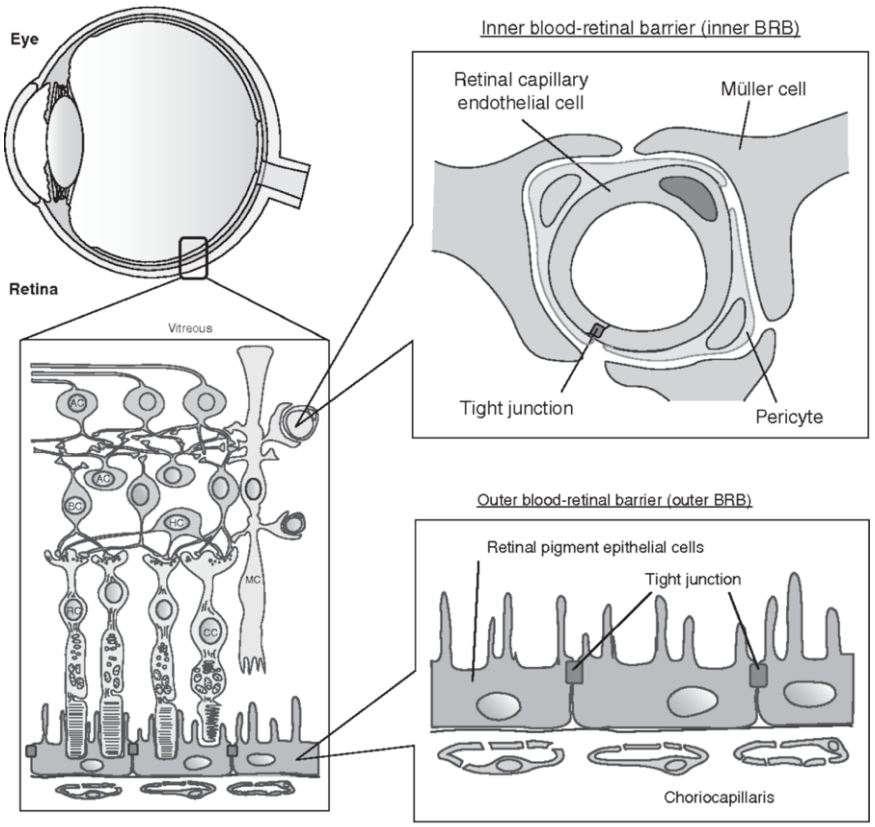

Fig. 8

Fig. 8 – Retinal barriers (from Hosoya et al. 2011) (*254*). The inner blood-retinal barrier is located below the GCL, and is formed by the tight junction between endothelial cells and the foot processes of astrocytes and MGCs. The outer blood-retinal barrier, instead, consists of tight junctions between the RPECs and the choroidal capillaries. Additionally, adherens junctions between MGCs and photoreceptors are also present.

Not all cell types are characterized by the same integration efficiency. As an example, NPCs can migrate extensively, even when transplanted intravitreally; however, they very rarely manage to differentiate into mature retinal cell types (*255, 256*). On the contrary,

RPCs are exceptionally efficient at differentiating into retinal neurons, but their migration and integration capability remains very limited (*117, 118, 187, 257*).

In general, it is reasonable to hypothesize that the beneficial outcomes of cell-based therapies could be higher if a larger percentage of the transplanted cells were incorporated into the host tissue.

3.4.1 Reactive gliosis

In addition to the presence of the outer and inner limiting membranes, migration of transplanted cells in the damaged retina is further impeded by reactive gliosis (*258*).
Reactive gliosis is a process that accompanies tissue injury and inflammation. Moreover, there's evidence suggesting that it can be further promoted by the transplantation procedure itself, especially in the case of intravitreal injection. This occurs in response to transplantation of multiple cell types, including MSCs, iPSCs, neuronal cells and photoreceptor precursors.

Reactive gliosis is characterized by a number of events that include: up-regulation of intermediate filaments; macrophage recruitment; microglia accumulation; and deposition of chondroitin sulfate proteoglycans (CSPGs) (*259, 260*).
CSPGs are molecules of the extracellular matrix (ECM) that consist of a protein core to which glycosaminoglycan (GAG) side chains are

attached. The length, number and sulfation degree of GAG chains is variable.

During development, CSPGs contribute to the regulation of pattern cell migration and axonal path-finding. In the adult CNS, they are involved in numerous processes, such as migration, adhesion and receptor binding. In general, they strongly limit cell plasticity and they have potent inhibitory effects with respect to both CNS regeneration and migration/integration of transplanted cells (*261, 262*).

Inhibition of reactive gliosis is critical for the success of cell-based therapies. Indeed, it has already been established that adjuvant anti-inflammatory therapy and local degradation of the ECM can significantly improve migration and survival of transplanted cells. CSPG activity, in particular, can be inhibited using the chondroitinase ABC (ChABC) enzyme.

ChABC selectively cleaves GAG chains from the protein core, thereby markedly reducing the inhibitory effects of CSPGs (*120, 263*). This not only results in enhanced axonal regeneration, but also facilitates transplanted cell migration (*264, 265*). Indeed, ChABC has been shown to promote synaptogenesis between transplanted photoreceptors and the host retina (*266*).

In other words, ChABC could represent a valuable tool to be incorporated in repair strategies, and to be used in combination with different approaches to achieve the greatest regeneration possible.

CHAPTER 4: Chemokines and their receptors

4.1 Chemokine structure and classification

Chemokines are small peptides of about 8-14 kDa that act as "chemotactic cytokines". They are crucially important for the regulation of leukocyte growth, maturation, differentiation and recruitment.

Chemokines have been classified into four families based on the relative position of their highly conserved cysteine residues (*267*). These cysteine residues pair up to form disulphide bonds that contribute to the stabilization of the typical Greek-key three-dimensional shape of chemokines.
With the exception of the C-chemokines (which contain a total of two cysteine residues), members of all other families contain four cysteines. Depending on the relative position of the N-terminal ones, they are classified into: (1) CC-chemokines (cysteines are adjacent to one another); (2) CXC-chemokines (cysteines are separated by a single amino acid, X); (3) CX3C-chemokines (cysteines are separated by three amino acids, X3) (Fig. 9A). Depending on the nature of the intercalating amino acid, CXC-chemokines can be further classified into neutrophils- or lymphocytes- chemoattractants.

Overall, chemokines are highly basic proteins, which makes them prone to bind to negatively-charged molecules. As a consequence,

they strongly interact with heparin and heparan sulfates, present in the extracellular matrix (ECM) and on the surface of endothelial cells (*268*). Chemokine retention and immobilization in the ECM creates a local concentration gradient, with the highest chemokine concentration close to the original release site (*269*). Such concentration gradient is responsible for guiding directed leukocyte migration.

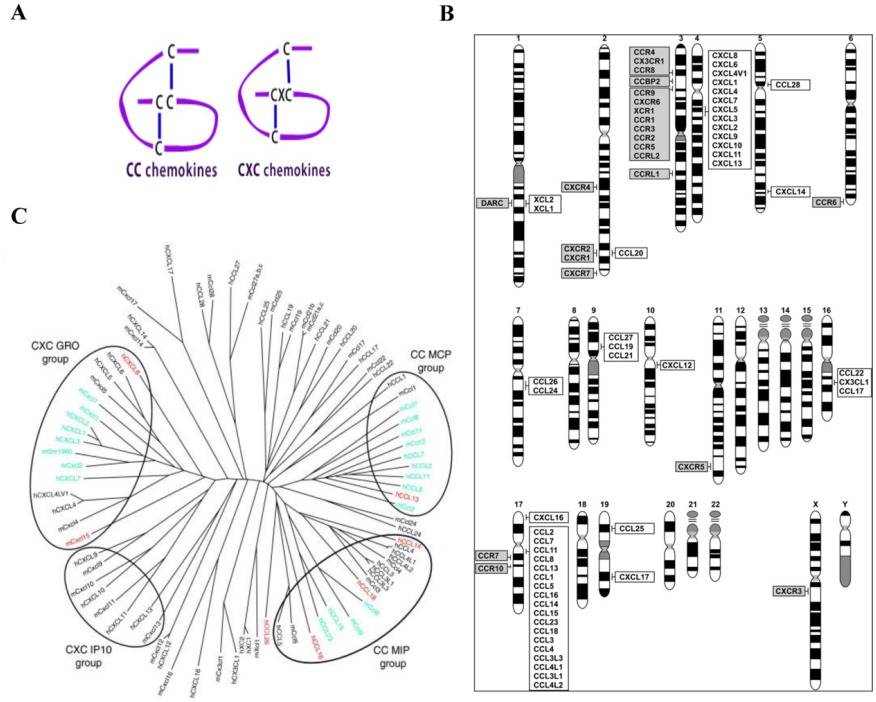

Fig. 9

Fig. 9 – Chemokine structure and evolution. (A) Relative position of the conserved cysteine residues in the chemokines of the CC and the CXC families. In the former, the two N-terminal cysteines are adjacent; in the latter, they are separated by a single amino acid, X. **(B)** Chromosomal map of the human chemokine and chemokine receptor genes (from Zlotnik & Yoshie, 2012) (*270*). The locations of the chemokines genes are highlighted in white boxes, whereas those of the chemokine receptors are in grey. Inflammatory CXC chemokines are concentrated on chromosome 4, while inflammatory CC chemokines are mainly

found on chromosome 17. **(C)** Sequence relationship analysis of the human (h) and mouse (m) chemokines (from Zlotnik et al., 2006) (*267*). The four groups of chemokines with a common evolutionary origin are highlighted by dark circles. Red letters indicate proteins that are found only in one species, but not in the other. Blue letters indicate proteins for which the relationships have a level of uncertainty.

4.2 Homeostatic *vs* inflammatory chemokines

The primary role of chemokines is to provide cues for the directed movement of immune system cells during development, homeostasis and inflammation. Indeed, based on their expression patterns and function, chemokines can be divided into two broad families.
On the one side, there are the homeostatic chemokines; on the other side, the pro-inflammatory ones. It is however important to stress that the distinction between homeostatic and inflammatory chemokines is not absolute: some inflammatory chemokines may have homeostatic functions, and vice-versa.

Homeostatic chemokines are involved in tissue maintenance and in the organization of the immune system. They are expressed in specific sites, and in the absence of activating stimuli. They can be regarded as "master regulators" of the movement and localization of lymphocyte and dendritic cell subsets in the body (*267, 271*).

Inflammatory chemokines, instead, are secreted exclusively in response to tissue injury and/or inflammation. They are involved in the regulation of leukocyte migration and recruitment.

While genes coding for homeostatic chemokines are sparsely located in the genome, the vast majority of the inflammatory genes map to two discrete chromosomal sites, one for CC chemokines and one for the CXC ones (*270, 272*). Based on phylogenetic, CC and CXC clusters can be further subdivided into four groups with a common evolutionary origin (Fig. 9B). The CC cluster, located on the human chromosome 17, contains the monocyte chemotactic protein (or MCP) and the macrophage inflammatory protein (or MIP) groups; the GRO and the IP-10 groups of CXC chemokines, instead, are found in the human chromosome 4 (*270*). While molecules belonging to the GRO cluster are mostly attractants for neutrophils, MCP and MIP proteins are responsible for the recruitment of several leukocytes, including monocytes, T cell subsets and eosinophils (*273*).

Chemokines have been implicated in the pathophysiology of several diseases, including inflammation, cancer, autoimmune and infectious diseases (*267, 274*). Inflammation-dependent increases in chemokine secretion have been detected in most organs, including the skin, brain, lungs, and gastro-intestinal tract. Such increases occur in response to bacterial products (e.g. lipopolysaccharides), viral infection, or the secretion of early pro-inflammatory cytokines (such as *Interleukin-1β - Il1-β -* or *Tumor necrosis factor-α - Tnf-α)* (*275*). Heightened chemokine levels are responsible for the selective recruitment of leukocytes into inflamed tissue. Importantly, each disease has a characteristic profile of secreted factors; in this way, a

"customized" response can be established, fine-tuning the subgroups of recruited leukocytes (*276*).

4.3 Chemokine receptors

Chemokines bind to seven transmembrane, class A G protein-coupled receptors (*277*). Homeostatic chemokines, in general, exhibit a rather restricted ligand usage, with only one or two chemokines binding to a given receptor. Inflammatory chemokine receptors, instead, display a high level of promiscuity: a given receptor can be engaged by several ligands, and a given ligand can interact with multiple receptors (*270*). However, CC and CXC receptors can exclusively bind to CC and CXC chemokines respectively. Such specificity can be most likely explained by the differences that exists between CC and CXC molecules at level of their quaternary structures (*278*).

Ligand-mediated activation of chemokine receptors results in the regulation of numerous processes, including cell migration, survival, growth, proliferation, and cytokine release (*268*). Members of the Ras and Rho families are also activated, contributing to the remodeling of the actin cytoskeleton and to the control of focal adhesion and cell motility (*279*).

So far, 18 functionally signaling chemokine receptors have been described in human and mouse. Just like their ligands, receptor genes

also form clusters. However, in contrast to inflammatory chemokines, they are considerably better conserved among species, including mouse and human (*272*).
Additionally, five atypical "scavenger" or "decoy" receptors have been identified, namely DARC, D6, CXCR7, CCRL1 and CCRL2 (*270*). They are able to bind to a large number of ligands, but do not activate intracellular cascades. In other words, they are non-signaling molecules that function as "sinks", removing chemokine from the environment, and therefore avoiding their excessive build-up. DARC, for instance, can bind several CC and CXC inflammatory chemokines; D6, instead, can only respond to inflammatory CC ligands. CCRL1 and CCRL2 differ from all other scavenger receptors as they are the only ones that can sequester homeostatic chemokines.

In addition to chemokine "scavenging", receptor signaling can be dampened by some chemokines acting as antagonists. Ligands of the CXCR3 and CCR3 receptors represent the most prominent example. In fact, they are reciprocally antagonists, meaning that CXCL9, CXCL10 and CXCL10 can inhibit CCR3 activity, whereas CCR3-ligands are natural antagonists for CXCR3 (*280*). Such balancing system makes perfect sense considering that CXCR3 is expressed by T helper 1 (Th1) cells, whereas CCR3 is present on T helper 2 (Th2): in this way, CXCR3- and CCR3-ligands can create microenvironments that favors either the Th1 or the Th2 cell differentiation respectively (*281*).

Chemokine receptor expression is highly heterogeneous. Some receptors are present only on a restricted number of cell types, whereas others are more widely expressed. CXCR1, for instance, is almost exclusively present on neutrophils, while CCR2 is expressed on monocytes, T cells, natural killer cells, dendritic cells, and basophils (*268*). Furthermore, their expression can be constitutive or inducible. As an example, CCR2 levels on lymphocytes are appreciable only after stimulation by interleukin-2 (*282*).
Generally, expression of homeostatic chemokine receptors is constitutive, and restricted to specific cell types or organs. Inflammatory receptors expression, instead, is considerably more heterogeneous, variable, and responsive to external stimuli (*270*).

4.4 Of mice and men: chemokine evolution and conservation across species

Homeostatic chemokines' structure and function are very well conserved across species. Inflammatory chemokines, instead, are one of the most rapidly changing proteins of the genome. This is due to the strong positive selective pressure that they are subjected to, which makes them evolve more rapidly than most other genes (*267, 272, 283*).
Furthermore, clusters of chemokine genes have been duplicated during the course of evolution (*272, 276*). Following duplication, two copies of the same gene can evolve independently and acquire

distinct functions; this most likely contributed to the prominent promiscuity of the ligand-receptor relationships.
Importantly, some of these duplication events have occurred recently (in evolutionary terms), i.e. after the branching of human and mouse. As a consequence, some chemokines have evolved independently in the two species. In other words, mouse and human chemokines do not always correspond well (*276*) (Fig. 9C).

In particular, three main differences can be highlighted. First, genes that appear to be very similar can have markedly different functions (*284*). Second, a given chemokine can be represented by more than a single orthologue in the other species. Third, some ligands exist in one organism, but not in the other. Ccl12, for instance, exclusively exists in mouse. On the contrary, CCL13 and CCL14 are only present in human. This probably is the result of diverse pathogen-driven selective pressures (*267, 270*).
For these reasons, care must be taken when extrapolating experimental results and conclusions based on the investigation of chemokines from mouse to humans.
Nonetheless, the mouse remains an extremely valuable model, and can definitely be used for the study of stem cell migration for the optimization of therapeutic approaches.

AIM OF THE STUDY

AIM OF THE STUDY

The overall aim of the study was to address the problem of inadequate migration of stem cells transplanted into the damaged and/or degenerating retina (Fig. 10). In particular, we decided to focus on mouse [redacted] and we tackled the following main objectives:

[redacted]

The ultimate goal was to improve the [redacted] responsiveness of transplanted [redacted], and, as a consequence, their migration and integration into the host tissue.

Fig. 10 – A strategy to improve migration in the retina. . The ultimate goal is to improve transplanted cells, and, as a consequence, their migration and integration into the host tissue.

RESULTS

PART I: Identification of [redacted] towards the damaged retina

Soluble factors released during retinal degeneration [redacted]

Tissue injury and inflammation have been extensively described to induce the release of chemotactic factors (*267, 270*). For this reason, we hypothesized the peak of retinal inflammation to be concomitant with the maximum secretion of molecules able to [redacted] In order to identify such time window, we analyzed expression of the *Il1-β* pro-inflammatory cytokine at multiple time points along the process of retina degeneration (Fig. 11). In accordance to previously published studies (*29, 31*), we found that *Il1-β* expression peaked 24h post-damage in the NMDA-induced model of degeneration (Fig. 11A), and at P18 in the *rd10* mouse (Fig. 11B). The peak in *Il1-β* mRNA was indicative of the occurrence of a strong, damage-dependent inflammatory response. Inflammation subsided over time, and it reached low levels one month post-NMDA damage (Fig. 11A) and at six months of age for the *rd10* mice (Fig. 11B).

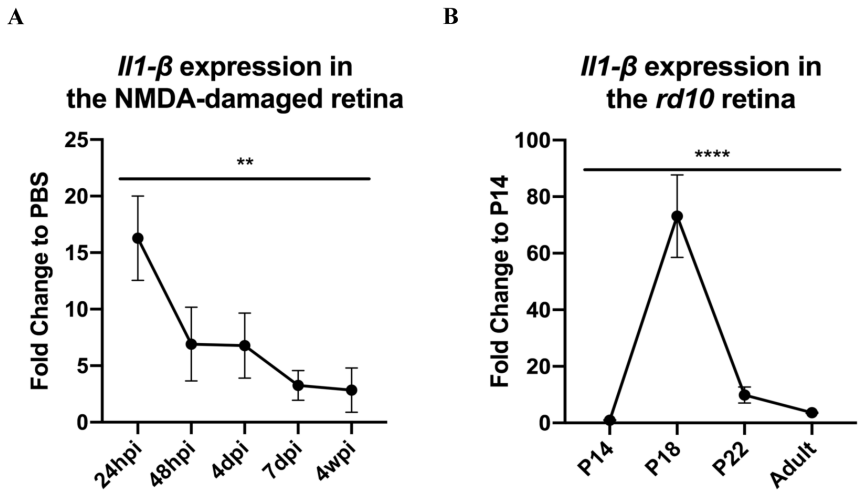

Fig. 11

Fig. 11 - Retinal damage is associated with an acute peak in expression of the pro-inflammatory cytokine *Il1-β*. qRT-PCR of *Il1-β* levels in the **(A)** NMDA-damaged retina (24 hpi, 48 hpi, 4 dpi, 7 dpi, 4 wpi) and in the **(B)** *rd10* retina (P14, P18, P22, adult). Transcript levels are expressed as fold-changes to control (PBS-injected or P14) retinae. Data is presented as mean ± SEM from n ≥ 3 independent experiments. One Way Anova was used for statistical analysis.

Next, we investigated whether damage-dependent inflammation would indeed [redacted] To do so, we performed a series of chemotactic assays using *ex vivo* cultured mouse retinae (Fig. 12). Based on our findings (Fig. 11A-B), we decided to focus on specific time points, i.e. 24 hpi for the NMDA-damage and P18 for the *rd10* mouse. Results from chemotactic assays revealed [redacted], as compared to the PBS-injected controls (Fig. 13A-B). A remarkably

similar phenotype was also observed in the case of the *rd10* model of RP (Fig. 13C-D).

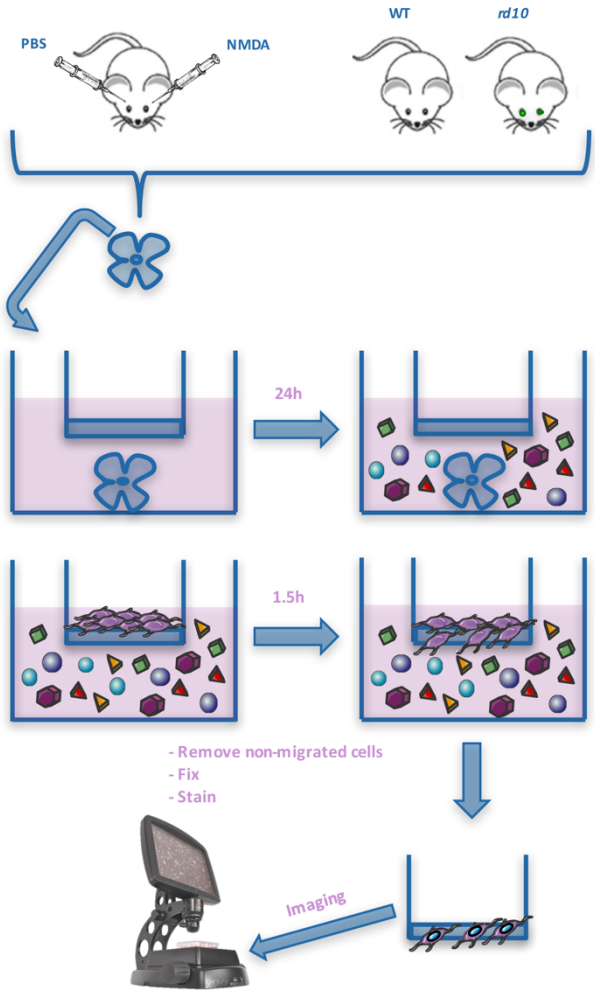

Fig. 12

Fig. 12 - Experimental scheme of chemotactic assays. WT mice received intravitreal injection of NMDA to induce retinal degeneration; the contralateral eye was injected with PBS, as a control. PBS/NMDA-injected animals were sacrificed 24 hpi, while *rd10* mice (and their age-matched WT controls) were sacrificed at P18. Retinae were then cultured for 24h in SF medium. At the moment of the assay, a suspension of $2*10^5$ MSC in SF medium was seeded in the upper chamber for 1.5h. Following incubation, non-migrated cells were removed. Migrated cells stuck in the porous membrane of the transwell were stained with DAPI, imaged and quantified.

Fig. 13 - soluble factors released during retina degeneration. (A) Quantification of Number of migrated cells is expressed as fold-change to control (PBS-injected) retinae. Data is presented as mean ± SEM from n ≥ 3 independent experiments. Mann-Whitney test was used for statistical analysis. **(B)** Representative DAPI-stained fields from transwell assays performed with conditioned medium from PBS- (up) or NMDA- (down) injected retinae. **(C)** Quantification of towards the conditioned media from WT- or *rd10* P18 retinae. Number of migrated cells is expressed as fold-change to control (WT) retinae. Data is presented as mean ± SEM from n ≥ 3 independent experiments. Mann-Whitney test was used for statistical analysis. **(D)** Representative DAPI-stained fields from transwell assays performed with conditioned medium from WT (up) or *rd10* (down) P18 retinae.

Given the high structural and functional similarity that exists among injury-dependent molecules in mouse and human, we then decided to explore whether We divided the central part of retinae from deceased human donors into quarters. For each of the experiments, a quarter was cultured in control medium, while another one was cultured in medium containing NMDA (1mM). We also received retinae from patients affected by RP; we could therefore test in this degenerative context as well. Analogously to what observed for the mouse retina, chemotactic assays showed that This applied both to the NMDA-damage (Fig. 14B-C) and to the RP (Fig. 14D-E) degenerative models.

To summarize, our results indicate that retinal damage is associated

Fig. 14 - soluble factors released by the damaged human retina. (A) Experimental scheme. The central part of the retina was divided into quarters. One of them was cultured in control medium, while another one was cultured in medium containing 1mM NMDA. Similarly, a quarter from a healthy control and a quarter from a RP retina were cultured in parallel. After 24h, the conditioned medium was collected and used to perform chemotactic assays. **(B)** Quantification of towards the conditioned media from human retinae cultured for 24h in control medium (healthy) or in medium containing NMDA. Number of migrated cells is expressed as fold-change to control (healthy) retinae. Data is presented as Min to Max boxes (with line at median) from n ≥ 3 independent experiments. Mann-Whitney test was used for statistical analysis. **(C)** Representative DAPI-stained fields from transwell assays performed with conditioned medium from healthy (up) or NMDA-damaged (down) human retinae. **(D)** Quantification of towards the conditioned media from healthy and RP human retinae cultured for 24h. Number of migrated cells is expressed as fold-change to control (healthy) retinae. Data is presented as Min to Max boxes (with line at median) from n ≥ 3 independent experiments. Mann-Whitney test was used for statistical analysis. **(E)** Representative DAPI-stained fields from transwell assays performed with conditioned medium from healthy (up) or retinitis pigmentosa (down) human retinae.

Specific subsets of inflammatory during retina degeneration

In order to identify the we profiled inflammatory in retinal lysates. We decided to focus on the two largest and most extensively characterized families of Compared to their control counterparts, both NMDA-

damaged (Fig. 15A) and *rd10* (Fig. 15B) retinae showed

Fig. 15 - Retinal damage

Data is presented as mean ± SEM from n = 2 independent experiments. **(B)**

Data is presented as mean ± SEM from n = 2 independent experiments.

Results from the cytokine arrays were validated by gene expression analysis

Fig. 16 - Retinal damage

(A) NMDA-damaged (24 hpi) and **(B)** P18 *rd10* retinae.

Data is presented as mean ± SEM from n ≥ 3 independent experiments. Mann-Whitney test was used for statistical analysis.

qRT-PCR analysis was also performed at different time points along the process of retinal degeneration (Fig. 17). Interestingly, we found that [redacted] followed a trend that was remarkably similar to that of *Il1-β (Fig. 18; Fig. 19)*. In other words, [redacted] peaked with the inflammatory response, and decreased over time, in parallel with the decrease in tissue inflammation.

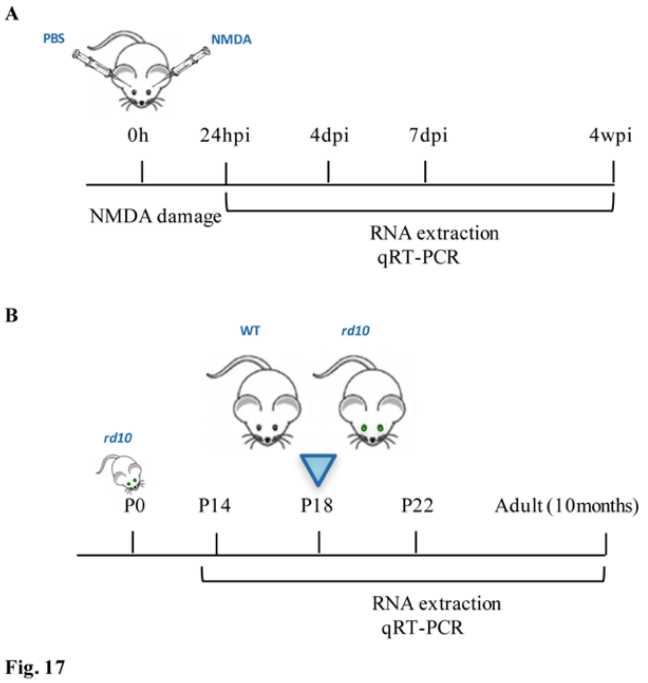

Fig. 17

Fig. 17 - Experimental set-up of the time course qRT-PCR analysis. (A) For the NMDA-damage, samples were collected 24 hpi, 48 hpi, 4 dpi, 7 dpi and 4 wpi. PBS-injected retinae were used as a control. **(B)** For the *rd10* model of RP, samples were collected at P14, P18, P22 and at 6 months of age (adults). P18 WT retinae were used as a control.

Fig. 18 - NMDA-damage is associated with time-dependent inflammation and Time course analysis of *Il1-β* and of **(B)** transcript levels in NMDA-damaged retinae (24 hpi, 48 hpi, 4 dpi, 7 dpi, 4 wpi). Transcript levels are expressed as fold-changes to control (PBS-injected) retinae. Data is presented as mean from n ≥ 3 independent experiments.

Fig. 19 - Retinal degeneration in *rd10* mice is associated with time-dependent inflammation and . Time course analysis of *Il1-β* and of **(A)** and **(B)** transcript levels in *rd10* retinae (P14, P18, P22, adult). Transcript levels are expressed as fold-changes to P14 retinae. Data is presented as mean from n ≥ 3 independent experiments.

Gene expression analysis was also performed on cultured human retinae, both in the case of NMDA-damage and in that of RP (Fig. 20A-C). Encouragingly we could detect an inflammatory response in both models, as indicated by the upregulation of *IL1-β and TNF-α* pro-inflammatory markers (Fig. 20A). Inflammation was accompanied by

Fig. 20 - Human retinal damage is associated with inflammation and . qRT-PCR of pro-inflammatory cytokines *IL1-β* and *TNF-α* **(A)**, **(B)** and **(C)** levels in healthy, NMDA-damaged and RP human retinae, cultured for 24h. Transcript levels are expressed as fold-changes to the healthy controls. Data is presented as mean ± SEM from n ≥ 3 (NMDA-damage) or n = 2 (retinitis pigmentosa) independent experiments. Mann-Whitney test was used for statistical analysis.

To summarize, proteomic screens and qRT-PCR analysis showed consistently higher levels of multiple inflammatory [redacted]

[redacted] e could identify several potential ligands-receptor chemotactic axis, including: [redacted]

Fig. 21 - [redacted]

To confirm that the observed phenotype was mediated by the identified signaling axis, we tested [redacted]

In the context of both NMDA- (Fig. 22A-B) and the RP- (Fig. 23A-B) induced degeneration, we found that [redacted]

[redacted]

Fig. 22 - [redacted] towards NMDA-damaged retinae [redacted]. (A) Quantification of [redacted] towards the conditioned media from NMDA-damaged retinae (24 hpi) in the presence of [redacted] Number of migrated cells is expressed as fold-change to control (vehicle - DMSO). Data is presented as Min to Max boxes (with line at median) from n ≥ 3 independent experiments. Mann-Whitney test was used for statistical analysis. **(B)** Representative DAPI-stained fields from transwell assays assessing [redacted] towards NMDA-damaged retinae (24 hpi) in the presence of DMSO (vehicle), [redacted]

Fig. 23 - [redacted] towards P18 *rd10* retinae [redacted]. (A) Quantification of [redacted] towards the conditioned media from P18 *rd10* retinae in the presence of [redacted] Number of migrated cells is expressed as fold-change to control (vehicle - DMSO). Data is presented as Min to Max boxes (with line at median) from n = 3 independent experiments. Mann-Whitney test was used for statistical analysis. **(B)** Representative DAPI-stained fields from transwell assays assessing [redacted] towards P18 *rd10* retinae in the presence of DMSO (vehicle), [redacted]

Endogenous expression profile of [redacted]

In accordance with published literature (*286, 287*), we found that [redacted] express [redacted] at an almost negligible level when compared to the very well-characterized [redacted] marker *Thy* (Fig. 24A).

Indeed, we also analyzed levels of cells surface [redacted] expression by FACS, and we found them to be extremely low (Fig. 24B). Only a small percentage of the population was positive for [redacted] represented the only notable exception, as it was expressed by the majority of the cells (>80%).

In other words, [redacted] displayed a heterogeneous profile with respect to [redacted] receptor expression. Actually, it could be concluded that their repertoire of functional [redacted] is quite limited.

Fig. 24 - [redacted] endogenous mRNA and cell surface expression of [redacted] (A) qRT-PCR of endogenous [redacted] levels of expression in [redacted] Transcript levels are expressed as fold-change to Thy. Data is presented as mean ± SEM from n = 3 independent experiments. **(B)** FACS analysis of endogenous [redacted] protein levels at the cell surface of [redacted] Results are expressed as percentage of positive cells. Data is presented as mean ± SEM from n = 3 independent experiments.

PART II: [redacted] towards the damaged retina *ex vivo*

Generation and characterization of [redacted] lines [redacted]

After identifying specific subsets of [redacted] whose expression and secretion were increased during retinal degeneration, we [redacted] their cognate [redacted]. Based on our results, we decided to proceed with the following [redacted] (Fig. 25A). [redacted] lines were generated via [redacted] and characterized using multiple, complementary approaches (Fig. 25-27).

Fig. 25 - Generation of [redacted] (A) [redacted]

Firstly, we ensured that [redacted] were upregulating the [redacted] at the mRNA level (Fig. 25B). Secondly, we performed immunostaining to confirm the expression of the GFP marker and of the HA-tagged [redacted] at the protein level (Fig. 26). Thirdly, we checked for the presence of the [redacted] at the cell surface by FACS (Fig. 27A). Interestingly, despite the dramatic upregulation of [redacted] expression (Fig. 25B), the percentage of positive cells generally remained below 50% [redacted] represented notable exceptions. The high percentage of [redacted] cells was not surprising, as the majority of [redacted] endogenously (>80%; Fig. 24B). Nonetheless, the increase in the number of [redacted] cells was particularly remarkable (<400-fold).

Finally, we ensured that the [redacted] were functional by testing their migratory response towards a defined chemokine gradient (Fig. 27B). In this case, the bottom well was filled with SF medium containing 50 ng ml^{-1} of a specific chemokine. We tested the following [redacted] chemokine combinations: [redacted] In all cases, we found that [redacted]

[redacted] migrated significantly more than their WT counterparts (Fig. 27B), which indicated that the exogenously expressed [redacted] were able to better response to stimulation with their cognate ligands.

Collectively, our results indicate that [redacted] exogenously expressed relatively high levels of the [redacted] that such [redacted] were correctly localized at the cell surface, and that they were functional.

Fig. 26 - [redacted] express the GFP and the HA tag at the protein level. Representative immunofluorescence staining of [redacted] to verify expression of the eGFP (green) and of the HA (red) tags.

Fig. 27 - [redacted] show increased levels of functional [redacted]

Results are expressed as percentage of positive cells. Data is presented as mean ± SEM from n ≥ 3 independent experiments. Two-tailed Student's T-test was used for statistical analysis. **(B)** Quantification of [redacted] towards a concentration of 50 ng ml^{-1} of [redacted] from transwell-based assays. Number of migrated cells is expressed as fold-change to control (WT-MSC). Data is presented as mean ± SEM from n ≥ 3 independent experiments. Mann-Whitney test was used for statistical analysis.

[redacted] towards the damaged retina *ex vivo*

Next, we investigated [redacted] towards the cocktails of soluble factors secreted during retinal degeneration. To do so, we tested [redacted] towards the conditioned medium from *ex vivo* cultured mouse retinae. Our results showed that [redacted] (Fig. 28). This applied to both the NMDA-induced (Fig. 28A) and the RP (Fig. 28B) models of retinal degeneration.

Based on our findings, we decided to further proceed with the [redacted] lines. We opted for [redacted] rather than [redacted] on the basis of the following considerations: [redacted]

Fig. 28 - [redacted] migrate more efficiently towards the degenerating retina. **(A)** Quantification of [redacted] towards the conditioned media from NMDA-injected **(A)** or rd10 **(B)** retinae, from transwell-based assays. Number of migrated cells is expressed as fold-change to control (MSC-WT). Data is presented as mean ± SEM from n ≥ 3 independent experiments. Mann-Whitney test was used for statistical analysis.

We also tested [redacted] towards the NMDA-damaged and the RP-affected human retinae (Fig. 29A-C). In both cases, chemotactic assays clearly showed that exogenous expression of the [redacted] could significantly [redacted]

Fig. 29 - [redacted] more efficiently than their WT counterparts towards the degenerating human retina. Quantification of [redacted] towards the conditioned media from **(A)** NMDA-damaged and **(B)** RP human retinae, from transwell-based assays. Number of migrated cells is expressed as fold-change to control (WT-MSC). Data is presented as mean ± SEM from n ≥ 3 independent experiments. Mann-Whitney test was used for statistical analysis.

PART III: [redacted] towards the damaged retina *in vivo*

[redacted] towards the damaged retina *in vivo*

Results from our *in vitro* and *ex vivo* assays showed that [redacted] towards the degenerating retina [redacted] We therefore proceeded to test migration of these [redacted] lines *in vivo*.

As illustrated in Fig. 30A, we intravitreally transplanted 500'000 cells, 12h post-NMDA damage. After four days, animals were sacrificed and the percentage of GFP^+ [redacted] in the retina was quantified by flow cytometry.

We found that both [redacted] led to a significant increase in the percentage of GFP^+ [redacted] in the retina (Fig. 30B).

Fig. 30 - **towards the damaged retina *in vivo*. (A)** Experimental scheme. Eyes were damaged via NMDA-injection 12h prior to transplantation of either WT- or FACS analysis was performed 4 days after the transplant (4dpi). **(B)** FACS-based quantification of GFP^+ in transplanted retinae, 4 dpi. Results are expressed as percentage of total retinal cells. Data is presented as Min to Max boxes (with line at median) from $n \geq 3$ independent experiments. Two-tailed Student's T-test was used for statistical analysis.

towards the damaged retina *in vivo*

Since both *in vivo*, we decided to test would lead to a further increase in overall cell migration.

To do so, we generated a line. This was achieved via of , each (Fig. 31A). We ensured that our both Fig. 31B). Of note,

Fig. 31 - Generation of **(A)** double positive cells were isolated by FACS-sorting for eGFP and applying . **(B)** qRT-PCR showing expression of the (left) and (right) genes in the and in the corresponding lines (i.e. Transcript levels are expressed as fold-changes to GFP$^+$ Empty- control. Data is presented as mean ± SEM from n = 3 independent experiments. Two-tailed Student's T-test was used for statistical analysis.

We also confirmed that were expressing both the GFP and the HA tags (Fig. 32A). Lastly, we performed assays to ensure were indeed endowing cells with an improved ability to respond to a defined gradient (Fig. 32B).

displayed an increased towards the soluble factors released by the retina during NMDA- and RP-induced degeneration (Fig. 33A). Importantly, both was significantly higher for as compared not only to but also single-expressing lines.

Finally, we tested migration of the *in vivo*. We analyzed the percentage of GFP$^+$ by FACS, 4 dpi. We found the number of to be significantly higher not only of the empty vector (WT) control, but also of the single expressing (Fig. 33B).

Fig. 32 - [redacted] express GFP, HA-tag and functional [redacted] **(A)** Representative immunofluorescence staining of [redacted] to verify expression of the eGFP (green) and of the HA (red) tags. **(B)** Quantification of migrated [redacted] towards a concentration of 50 ng ml^{-1} of [redacted] from transwell-based assays. Number of migrated cells is expressed as fold-change to control (WT-MSC). Data is presented as mean ± SEM from n ≥ 3 independent experiments. Mann-Whitney test was used for statistical analysis.

Fig. 33 - [redacted] migrate more efficiently than [redacted] towards the degenerating retina *ex vivo* and *in vivo*. **(A)** Quantification of [redacted] towards the conditioned media from NMDA-injected or *rd10* retinae, from transwell-based assays. Number of migrated cells is expressed as fold-change to control (WT-MSC). Data is presented as mean ± SEM from n ≥ 3 independent experiments. Mann-Whitney test was used for statistical analysis. **(B)** FACS-based quantification of GFP^+ [redacted] in transplanted retinae, 4 dpi. Results are expressed as percentage of total retinal cells. Data is presented as mean ± SEM from n ≥ 3 independent experiments. Two-tailed Student's T-test was used for statistical analysis.

Our data indicates that double [redacted] both *ex vivo* and *in vivo*.

We then decided to investigate cell migration and integration in the long term. To do so, we sacrificed NMDA-damaged mice whose eyes had been transplanted with either [redacted] 4 wpi. Retinal flat mounts were prepared and stained for GFP (marking the genetically modified [redacted]) and βIII-tubulin, a neuron-specific marker expressed by ganglion cells and interneurons. We found that GFP^+ [redacted] could be detected in the tissue in the long term, as

exemplified in Fig. 34. The almost complete absence of βIII-tubulin$^+$ cells most likely is the result of the NMDA-induced apoptosis of ganglion cells and interneurons (Fig. 34).

Interestingly, we could not observe the presence of GFP$^+$ cells in areas that had not been visibly affected by the NMDA-damage and that contained a high number of βIII-tubulin$^+$ cells (Fig. 35). This indicated that [redacted] were capable of "sensing" the areas of damage, and selectively migrated towards them.

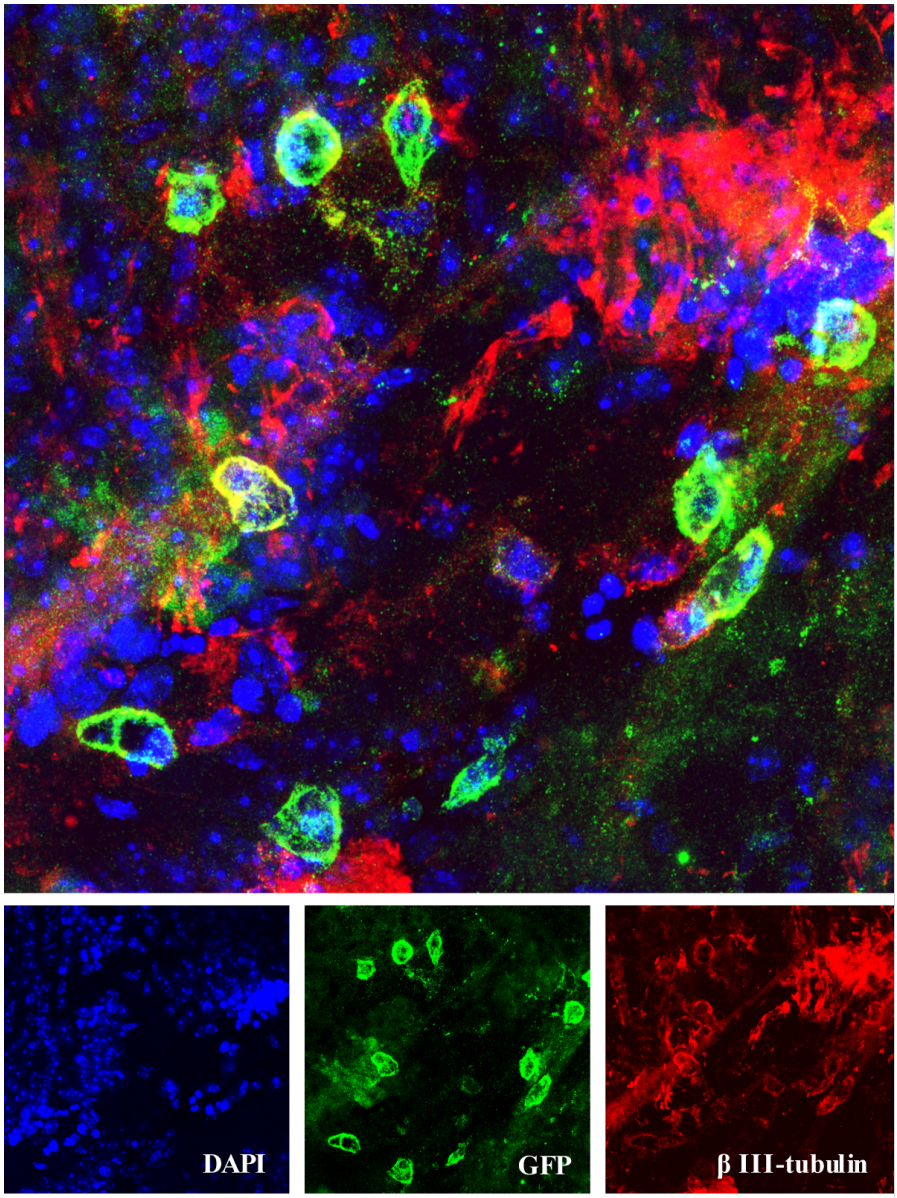

Fig. 34

Fig. 34 - Representative immunostaining of retinal flat mounts harvested from NMDA-damaged mice transplanted [redacted] βIII-tubulin (red) is a neuron-specific marker. The field displays a remarkable low density of βIII-tubulin^{+} neuronal cells, indicating that this specific area has been visibly affected by the NMDA-damage.

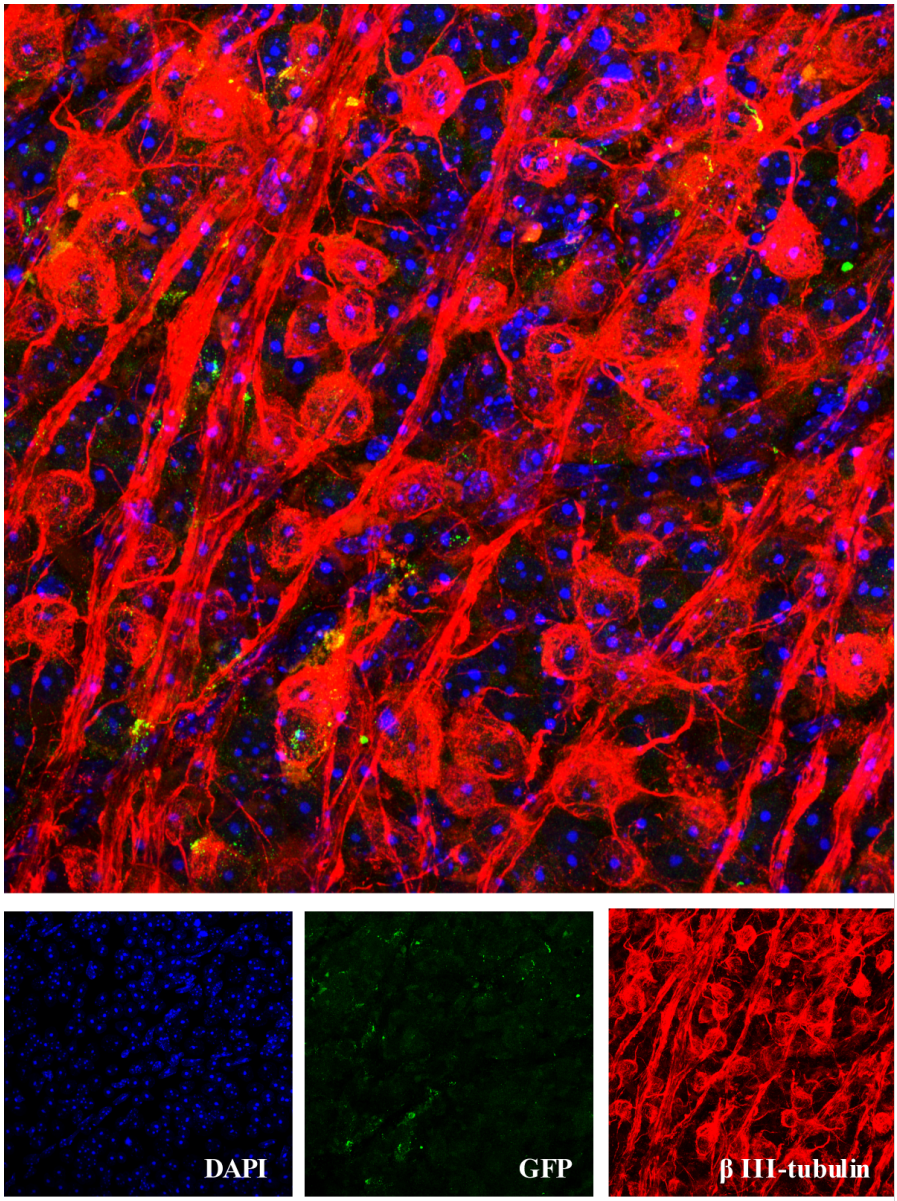

Fig. 35

Fig. 35 - Representative immunostaining of retinal flat mounts harvested from NMDA-damaged mice transplanted [redacted] The field displays a high density of βIII-tubulin^{+} (red) neuronal cells, indicating that this specific area has not been visibly affected by the NMDA-damage. [redacted]

To quantify the extent of the change in migratory capabilities, we decided to count the number of GFP$^+$ [redacted] in retinal sections prepared 4 wpi (Fig. 36). We still are in the process of gathering enough data as to make firm claims supported by solid statistical analysis. Nonetheless, our preliminary results indicate that the number of GFP$^+$ [redacted] tend to be higher than that of GFP$^+$ WT-[redacted] (Fig. 37).

In order to assess whether transplanted cells would undergo a change in their identity, we stained retinal sections for the neuron-specific marker βIII-tubulin, and counted the number of GFP$^+$/βIII-tubulin$^+$ cells. Most of the [redacted] that had reached the retinal layers were found to express βIII-tubulin (Fig. 38), which is indicative of a switch to a neuronal-like phenotype. Even though the absolute number of GFP$^+$/βIII-tubulin$^+$ cells tended to be higher in the retinae of mice transplanted with [redacted] (Fig. 38A), we were unable to observe any difference in the "transdifferentiation rate" or "TD", i.e. the percentage of the GFP$^+$/βIII-tubulin$^+$ cells over the total GFP$^+$ cells (Fig. 38B; [redacted] = 83,2% ± 0,2%; [redacted] = 86,7% ± 4,6%). A representative section from this experiment is presented in Fig. 39.

Fig. 36 – Representative immunostaining of retinal sections harvested from NMDA-damaged mice transplanted with either WT- (left) or [redacted] and sacrificed 4 wpi. [redacted] are GFP^+ (green). Higher magnification images from the white boxes are shown in the top-left or top-right corners.

Fig. 37 – Quantification of GFP^+ [redacted] found within the retinal layers of NMDA-damaged mice transplanted with either WT- (left) or [redacted] and sacrificed 4 wpi. Cells were counted in a minimum of ten sections, and in at least three random fields per section. Data is presented as mean ± SEM from n = 1 experiment. Representative fields from WT- and [redacted] transplanted retinae are shown in Fig. 36.

Fig. 38 – Quantification of βIII-tubulin$^+$ MSCs found within the retinal layers of NMDA-damaged mice transplanted with either WT- or [redacted] and sacrificed 4 wpi. Cells were counted in a minimum of ten sections, and in at least three random fields per section. Data is presented as mean ± SEM from n = 1 experiment. A representative field from [redacted] transplanted retinae is shown in Fig. 39. Results are presented either as **(A)** absolute number of GFP^+/βIII-tubulin$^+$ or as **(B)** "transdifferentation rate", i.e. as the percentage of the GFP^+/βIII-tubulin$^+$ cells over the total GFP^+ cells.

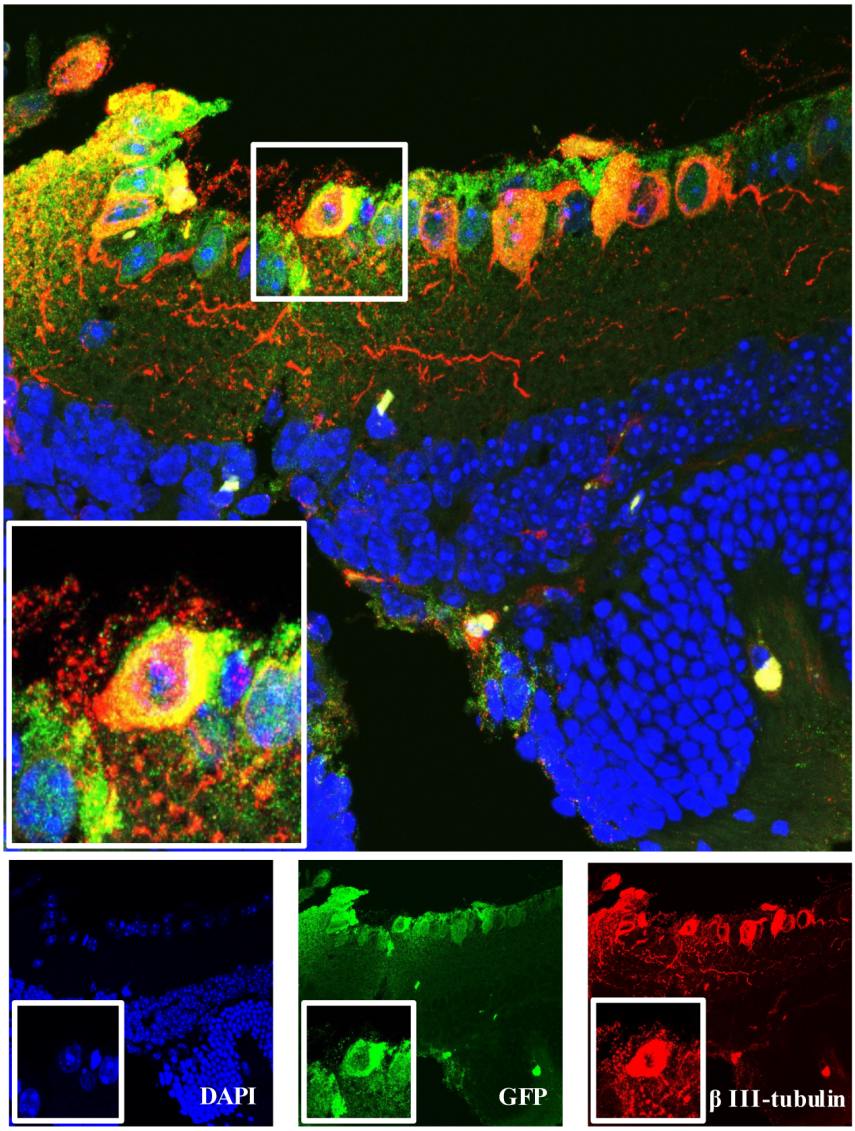

Fig. 39

Fig. 39 – Representative immunostaining of retinal sections harvested from NMDA-damaged mice

DISCUSSION

DISCUSSION

In this work, we have [redacted] both *ex vivo* and *in vivo*, via [redacted] has already been employed by other groups for stem cell therapy in different diseases, [redacted] Importantly, the chemotactic axis exploited in these studies were not always the same. For instance, [redacted] performed better than WT-[redacted] in the context of [redacted] however, they could not confer any advantage when transplanted into [redacted] In this case, [redacted] was able to improve [redacted]

Before selecting potential ligand(s)-receptor(s) signaling axis to be further investigated, we have therefore considered necessary to reveal the identity of the chemokines produced at the injury site. Eventually, we narrowed it down to the [redacted]

By doing so, we contributed to the generation of a more comprehensive understanding of the signaling pathways and cues involved in [redacted] during retinal degeneration.

We reported that NMDA-damaged and RP-affected retinae, both murine and human, were characterized by a strong inflammatory response, and by upregulation of several [redacted]

(Fig. 16, 20). The peak of [redacted] production occurred concomitantly to the peak in expression of pro-inflammatory markers (Fig. 11, 18, 19). Our observations are in accordance with published literature, as tissue injury has been strongly associated with the secretion of TNF-α and IL-1β. The concomitant release of inflammatory [redacted] can then induce the recruitment of leukocytes [redacted].

Compared to the mouse ones, NMDA-damaged human retinae seem to upregulate a broader spectrum of [redacted]

This could be explained by the fact that a 24h-long *in vitro* (rather than an injection-based *in vivo*) damage of the tissue might exacerbate chemokine release, generating some artefacts. Results from RP-affected retinae might be more reliable, since degeneration is induced by genetic mutation(s). However, we are still waiting for at least an additional RP sample in order to be able to draw more definite conclusions.

For the time being, we can state that both of the tested human models are characterized by consistent up-regulation of [redacted] Of note, human [redacted] correspond to the murine [redacted]. Importantly, [redacted] are included in the list of overlapping [redacted] suggesting that our strategy could be potentially applied to RP patients.

NMDA-damage and RP are associated with apoptosis of ganglion/amacrine neurons and photoreceptors respectively. Nonetheless, there is evidence that the inflammatory response of the retina is mainly orchestrated by MGCs, RPECs and activated microglia (*4*). For instance, as assessed by hybridization and immunohistochemical studies, [redacted] the *rd* mouse retina at P18 is mainly produced in the inner retinal layers, especially by MGCs and microglia cells (*6*). [redacted] is also released by cultured human RPECs upon exposure to TNF-α and IL-1β (*7, 8*). In other words, cytokine/chemokine-releasing cells are the same independently of the injury model and of the type of retinal neurons that undergo apoptosis. It is therefore not surprising that the subsets of upregulated chemokines we identified in NMDA-damaged and RP retinae were strikingly similar and largely overlapping. Indeed, the strong increase in [redacted] that we observed was also reported in other disease models, [redacted]

Crucially, the existence of these highly comparable, site- (rather than disease-) specific patterns of [redacted] upregulation would make our strategy widely applicable, [redacted]

The success of our approach is dependent on the secretion of [redacted] factors into the vitreous cavity. Importantly, this is known to happen during retinal degeneration in human patients (*14-17*). Indeed, there seems to be a correlation between the number of inflammatory cells recruited in the vitreous cavity and the visual

function of the patient: the higher the former, the lower the latter (*18*). For instance, [redacted]

Since inflammation tend to subside over time in our murine degenerative models (Fig. 11), it could be argued that an inflammation-dependent approach would have no validity for adult patients affected by genetic conditions with a relatively early onset (or that it would be only applicable during an extremely narrow time-window). What is important to stress, in this respect, is that inflammation seems to be chronic in human RP patients. In fact, even though stronger inflammatory reactions are generally found in younger patients with active disease processes, the inflammatory state continues even after photoreceptor loss (*18*). This is not to be underestimated, and it needs to be taken into account for the development and the optimization of therapeutic strategies. In particular, long-term, persistent inflammation means that the levels of chemokines released by the tissue will be elevated throughout the lifespan of RP-affected patients. This is consistent with our results, which showed that conditioned medium from the retina of elderly RP patients can strongly [redacted] (Fig. 14). In fact, the samples we received were all from patients that passed away [redacted] and therefore had already gone through the acute phase of photoreceptor loss.

We found that [redacted] possess a highly heterogeneous and quite limited repertoire of [redacted] (Fig. 24). For instance,

based on our FACS analysis, less than 1% of the cells are positive for [redacted] (<1%), and even a smaller percentage is positive for [redacted] (<0.5%). This is consistent with published literature (*2, 19*), and could provide an explanation for the low response of [redacted] to the damage-dependent chemokine gradient *in vivo*. The validity of the strategy presented in this study becomes clear in light of these considerations: in order to reach the injury site, [redacted] need to express the [redacted] that recognize the [redacted] produced there at sufficiently high levels. Since [redacted] hardly express any [redacted] or [redacted] it's not surprising that exogenous expression of these [redacted] can enhance their homing capabilities.

Analogously to that of [redacted] human [redacted] expression of [redacted] is also heterogeneous. However, they seem to generally express more [redacted] than murine ones. For instance, 40-70% of [redacted] have reported to express [redacted] [redacted] assays have shown that such [redacted] interact with their cognate [redacted] with the exception of [redacted] (*21*). In fact, intriguingly, [redacted] migration is not increased upon stimulation with the [redacted] ([redacted]. It's also enthralling to note that expression of [redacted] is clearly detectable by PCR, but that of [redacted] This further supports our decision to over-express [redacted]

It is also important to consider that [redacted] More specifically, prolonged *ex vivo* cell culturing and expansion can lead to substantial

downregulation of [redacted] Genetic modification of cultured [redacted] would allow to overcome the problem.

It could be reasonably argued that FACS-sorting of [redacted] subpopulations endogenously expressing [redacted] could represent a valid alternative [redacted] However, [redacted] offers two significant advantages: (1) [redacted]re considerably higher, which most likely means that cell responsiveness [redacted] (2) it will be easier to obtain a sufficiently high number of [redacted] cells as to adequately replace the lost/damaged ones. Indeed, there are some reports supporting the hypothesis [redacted] provide a sufficient number of number of viable cells *(1)*.

Interestingly, the fold-change increase in [redacted] expression (Fig. 25B) and its absolute expression levels (Fig. 25C) were of a smaller magnitude than those of the other tested [redacted] Nonetheless, the percentage of [redacted] was above 80% when assessed by FACS, which represented an approximately 400-fold upregulation with respect to [redacted] (Fig. 27A). This probably explains why [redacted] represented the [redacted] line with the highest migration capabilities *in vivo* (Fig. 30). Actually, *in vivo* [redacted] of the cells could most likely be further improved by more restrictive cell sorting prior to transplantation.

Ex vivo, [redacted] performance was equivalent to that of [redacted]

[redacted] and both of them performed slightly worse than [redacted] (Fig. 28). *In vivo*, however, [redacted] were not able to migrate as much as either [redacted] (Fig. 30). Such apparent contradiction could be due to additional effects played by the local microenvironment *in vivo* (*24*). We are currently unable to provide a definitive explanation. Nonetheless, our results are in line with a recent study showing that over-expression of [redacted] was unable to enhance [redacted] in the injured myocardium, despite the significant upregulation of [redacted] instead, displayed increased migratory capabilities, and their transplantation was [redacted]

Despite the promising results presented in this study, our strategy holds potential for further improvements. In particular, to generate [redacted] In a clinical setting, this would raise important concerns with respect to the risk of tumorigenesis. In fact, [redacted] randomly integrate into the genome, and can therefore lead to undesired, harmful mutations. Moreover, [redacted] would be maintained indefinitely by the cells, with unknown consequences. Considering that [redacted] might be dispensable once the cells reach the damage site, transient cell modification could represent a safer option.

[redacted]

[redacted]

To conclude, the identification of safer and less-invasive delivery strategies, coupled to the establishment of detailed procedures for the

generation of clinical-grade cells, will help overcome some of the major hurdles that currently hinder the translation of stem cell therapy approaches to the clinical setting.

Additionally, it is reasonable to hypothesize that our approach would lead to greater beneficial outcomes if adipose-derived (AD) [redacted] were used in spite of bone-marrow derived (BM-) ones. In fact, compared to [redacted] are characterized by higher proliferation rates and higher paracrine activity (*32, 33*). Moreover, they can be effectively isolated in high amounts with minimally invasive methods. Just like their BM-derived counterparts, they have a heterogeneous repertoire of [redacted]. However, the percentage of cells positive for [redacted] appears to be higher in [redacted]. This opens up the possibility that [redacted] may display better baseline migration capacities, in addition to having more potent neuroprotective effects. As a consequence, they might represent better candidates for the development of therapeutic approaches.

Lastly, it's appropriate to mention that even though mouse models of retina degeneration are very valuable for the development of cell-based therapeutic approaches, it could be extremely useful to further investigate our technology in non-human primates. In fact, translation from rodent models directly into humans might cause the underestimation of important issues, such as the anatomical and structural differences between species. As an example, rodent eyes are characterized by a large lens with a very small vitreous volume;

the human eye, instead, has a considerably larger vitreous cavity, with a small lens (*35*). This might significantly alter the dynamics of cell migration and integration. Therefore, transplantation methods developed for rodents might require further optimization prior to applicability to humans.

Importantly, all primate eyes are anatomically very similar, with comparable sizes and architectures. They also possess unique structures (such as the macula and fovea) that are not present in the murine retina (*36*). Furthermore, primates have immunological reactions that resemble those of humans more than rodents do; this is essential for the careful evaluation of possible adverse immune responses to grafts (*36*).

For these reasons, studies on non-human primate models could represent an important intermediary preclinical step, allowing for the meticulous assessment of the efficacy and the safety of cell therapy in the eye.

To summarize, the fundamental aim of this study was to address the problem of inadequate [redacted] of transplanted cells, with the final goal of improving the therapeutic outcome of stem cell therapy in the eye. To this end, we generated *ad hoc* engineered stem cell with improved responsiveness to retina-specific signals. The modified cells can more efficiently [redacted] the host tissue after transplantation, thanks to the engagement and the activation of the [redacted] by a subset of [redacted] that are released in a damage-dependent manner.

We also have some preliminary evidence suggesting that [redacted] can acquire a neuronal phenotype *in vivo* (Fig. 38-39). Indeed, the vast majority of the transplanted cells (>80%) were found to express βIII-tubulin, one month post-injection. Interestingly, [redacted] does not seem to alter the capacity [redacted] to acquire a neuronal phenotype, as exemplified by the fact that we could not detect any difference in the transdifferentiation rates of WT- and [redacted]. The observation that the absolute number of GFP^+/βIII-$tubulin^+$ cells is higher in mice transplanted with [redacted] reflects the increase in the total number of GFP[redacted] that are able to reach the retinal layers.

In addition to gathering further data to support our findings, we currently are evaluating whether transplantation of [redacted] can lead to increased retinal rescue, as compared to WT-[redacted]

If that was the case, transplantation of genetically engineered cells in the degenerating retina would stand as an efficient approach with an extremely high degree of adaptability and versatility. In fact, in addition to being suitable for patients with different types of retinopathies, it could potentially be applied not only [redacted], but to the all range of transplanted cell types. As a significant example, it could be employed to improve homing of retinal and/or photoreceptor precursors cells, which are inherently good at differentiating into mature retinal neurons, but display very poor migratory capabilities (*37-40*).

In conclusion, this study provides a possibly viable solution to the challenge of achieving effective delivery and engraftment at the site of injury.

Undoubtedly, there still is considerable work to be carried out. Nonetheless, our findings could eventually be integrated with alternative optimization strategies to make stem cell therapy in the eye a feasible and realistic option for the treatment of retinopathies, and for the achievement of visual restoration.

CONCLUSIONS

CONCLUSIONS

1. [redacted]Soluble factors released during retinal degeneration can [redacted]

2. Retinal degeneration is associated with a strong inflammatory response and with concomitant upregulation of specific subsets of [redacted]

3. Our findings apply both to gangliar/amacrine (i.e. NMDA-damage) and to photoreceptor (i.e. *rd10* mouse) degeneration, not only in rodent, but also in human models

4. *Ex vivo* [redacted] by inhibition of the [redacted]

5. The repertoire of [redacted] endogenously expressed by [redacted] is heterogeneous and quite limited

6. Over-expression of [redacted] enhances [redacted] towards the damaged retina *ex vivo*

7. [redacted] display an improved migratory phenotype towards the damaged retina *in vivo*

8. [redacted] display an even greater migratory phenotype, both *ex vivo* and *in vivo*

9. Transplanted [redacted] that reach the retinal layers are able to survive in the long-term, and

10. They start expressing the neuron-specific marker βIII-tubulin, indicating that they can acquire a neuronal-like phenotype

MATERIALS AND METHODS

MATERIALS AND METHODS

Cell and tissue culture

Bone marrow-derived [redacted]C57BL/6) were purchased from GIBCO (S1502-100) and maintained in DMEM/F-12-GlutaMAX supplemented with 10% fetal bovine serum (FBS), penicillin (100U ml^{-1}) and streptomycin (100µg ml^{-1}).

Mouse retinae were dissected and cultured in serum-free (SF) DMEM/F-12-GlutaMAX with penicillin (100U ml^{-1}) and streptomycin (100µg ml^{-1}).

Human retinae were dissected and cultured in SF Neurobasal A medium supplemented with GlutaMAX (0.5%), N2 (1x), B27 (1x), penicillin (100U ml^{-1}) and streptomycin (100µg ml^{-1}).

Animal care and treatment

Mice were maintained under a 12-hour light/ dark cycle with access to food and water *ad libidum*, in accordance with the Ethical Committee for Animal Experimentation (CEEA) of the Government of Catalonia. The CEEA of the Parc de Recerca Biomèdica de Barcelona (PRBB, Spain) reviewed and approved all animal procedures. Additionally, procedures and experiments were performed in accordance with the ARVO Statement for the Use of Animals in Ophthalmic and Vision Research, and with ARRIVE (Animal Research: Reporting of *In Vivo* Experiments) guidelines (*288*).

Male and female animals between 8-12 weeks were used for the study and assigned randomly to the various treatment groups. A minimum of three mice per treatment group was used. General anesthesia was induced when needed with intraperitoneal injection of ketamine (70 mg/kg) and medetomidine (10 mg/kg). Anesthesia was reversed with atipamezole (2 mg/kg). At endpoints, mice were euthanized using CO_2.

Retinal Damage and Cell Transplantation

Mice were anaesthetized and intravitreally injected with 2 µl of either NMDA (20 mmol μl^{-1}; Sigma) or PBS, as a control. Briefly, a 30-G needle was used to carefully make a small, punch incision at the upper temporal ora serrata. The 33-gauge needle of a Hamilton's syringe was then inserted into the incision, angled toward the optic nerve, to inject PBS or NMDA into the vitreous. The needle was left in place for a couple of seconds before being retracted to avoid reflux.

For cell transplantation, [redacted] were detached using Accutase (StemPro® Accutase® Cell Dissociation Reagent, Life Technologies™), counted and resuspended in PBS plus chondroitinase ABC (ChABC, 0.1 U μl^{-1}) at a concentration of 250'000 cells μl^{-1}. Adult mice that had received NMDA-damage were transplanted intravitreally with 2 µl of [redacted] (i.e. 500'000 cells), 12h post-damage. *Rd10* mice were transplanted with 1 µl of [redacted] subretinally (i.e. 250'000 cells) at P18.

Human retinae culture

Eye globes from donors whose cornea had been classified as non-suitable for transplantation were received from the "Banc d´Ulls per a Tractaments de Ceguesa" (BUTC). Explicit, written informed consent for the removal and use of the eye globes for diagnostic and research purposes was obtained from patients and/or relatives. All of the samples we received were from donors aged 65-90.

The retina was dissected employing a procedure and a set-up optimized in our laboratory in collaboration with "Centre d'Oftalmologia Barraquer". Briefly, the eye globe was placed in a holder that generated vacuum, thereby providing sufficient internal pressure as to perform the dissection. Cornea, iris and crystalline were removed performing an incision 6mm away from the Iris. This exposed the internal part of the eye globe, allowing to easily identify the retina, attached to the retinal pigmented epithelium (RPE). The vitreal excess was removed and the retina was separated mechanically from the RPE with the help of two forceps. The eye globe was then placed up-side-down in a sterile petri dish. In this way, the junction with optic nerve was exposed, and could be severed, thereby allowing to completely separate the retina from the rest of the eye globe. After the removal of the periphery and of the vitreal leftovers, the central part of the retina was cultured for 12-24h and then processed for experiments.

RNA extraction and quantitative real-time PCR (qRT-PCR)

RNA was extracted from dissected retinae using the RNA Isolation Mini kit (QIAGEN), according to the manufacturer protocol. RNA was reverse-transcribed with SuperScript III (Invitrogen). qRT-PCR reactions were performed using Platinum SYBR green qPCix-UDG (Invitrogen) in a LyghtCycler 480 (Roche) machine, according to the manufacturer recommendations. The oligoes used are listed in Table 2. qRT-PCR data was normalized to GAPDH expression. For each sample, we had at least a technical duplicate. A minimum of three independent experiments were averaged.

For the investigation of NMDA-damage, eye samples were collected 24 hours (24hpi), 48 hours (48hpi), 4 days (4dpi), 7 days (7dpi) or 4 weeks (4wpi) post-injection.
Rd10 mice were sacrificed at P14, P18, P22 and at 6 months of age (adults). To study gene expression in human retinae, RNA was extracted following 24 hours culturing in SF medium with or without NMDA (1mM).

RNA for the qRT-PCR analysis of cultured mMSCs was extracted from pelleted cells using the RNA Isolation Mini kit (QIAGEN). The oligoes used are also listed in Table 2.

Gene	Primer FW	Primer RV
[redacted]	[redacted]	[redacted]
[redacted]	[redacted]	[redacted]
[redacted]	[redacted]	[redacted]
[redacted]	[redacted]	[redacted]
[redacted]	[redacted]	[redacted]
[redacted]	[redacted]	[redacted]
[redacted]	[redacted]	[redacted]
[redacted]	[redacted]	[redacted]
[redacted]	[redacted]	[redacted]
[redacted]	[redacted]	[redacted]
[redacted]	[redacted]	[redacted]
[redacted]	[redacted]	[redacted]
[redacted]	[redacted]	[redacted]
[redacted]	[redacted]	[redacted]
[redacted]	[redacted]	[redacted]
[redacted]	[redacted]	[redacted]
[redacted]	[redacted]	[redacted]
[redacted]	[redacted]	[redacted]
[redacted]	[redacted]	[redacted]
[redacted]	[redacted]	[redacted]
[redacted]	[redacted]	[redacted]
[redacted]	[redacted]	[redacted]
[redacted]	[redacted]	[redacted]
[redacted]	[redacted]	[redacted]
[redacted]	[redacted]	[redacted]
[redacted]	[redacted]	[redacted]
[redacted]	[redacted]	[redacted]
[redacted]	[redacted]	[redacted]

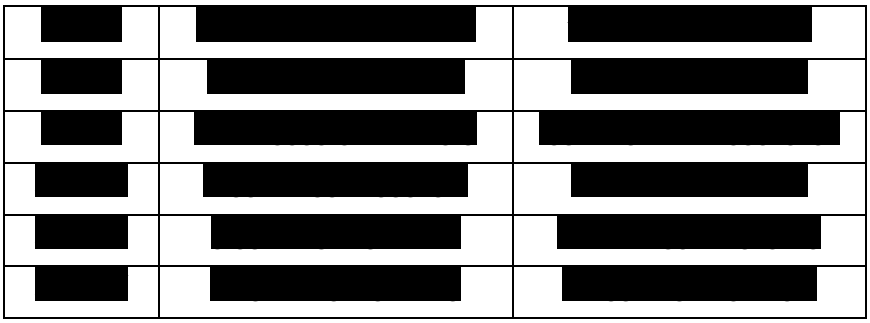

Table 2. Primers used for qRT-PCR analysis.

Chemotaxis assays

Chemotaxis assays were performed using transwell inserts (pore size, 8 μm, BD Biosciences - 353182) and 12-well culture plates.

To test migration towards defined [redacted] gradients, each lower chamber was loaded with 1.2 ml of SF DMEM/F-12-GlutaMAX medium with [redacted] or a combination of [redacted] (all 50ng ml^{-1}, Peprotech). To test migration towards control and damaged tissues, each lower chamber was loaded with 1.2 ml cell-free conditioned medium from either mouse or human retinae. For the NMDA-damage, mice were sacrificed 24 hpi; *rd10* mice were sacrificed at P18. Mouse and human retinae were cultured for 24 hours in SF DMEM/F-12-GlutaMAX and SF Neurobasal A (with or without 1mM NMDA) respectively.

The upper chamber of the insert was loaded with $2*10^5$ [redacted] in SF medium. The medium used to resuspend [redacted] was matched to

the medium in the bottom chamber: either DMEM/F-12-GlutaMAX (to test migration towards medium from mouse retinae) or Neurobasal A (to test migration towards medium from human retinae).
To test [redacted] impairment, [redacted] were incubated for 20min at 4°C with small molecule [redacted] antagonists, used as indicated Table 3.

Transwell plates were incubated for 1.5h at 37°C. Afterwards, non-migrated cells remaining on the upper surface of the inserts were removed with a cotton swab. Tranwells were then washed (PBS), fixed (4% paraformaldehyde - PFA, 10min) and stained with 5mg ml^{-1} 6-diamidino-2-phenylindole (DAPI, Sigma). For each insert, seven random field were imaged and analyzed. Cells were automatically counted using a custom-made macro for the ImageJ software (US National Institutes of Health, Bethesda, Md., USA; http://rsb.info.nih.gov/ij/).

Compound Name	**Catalogue Number (R&D Systems)**	[redacted]	**Working Concentration**
[redacted]	[redacted]	[redacted]	6 µM
[redacted]	[redacted]	[redacted]	25 µM
[redacted]	[redacted]	[redacted]	7 µM
[redacted]	[redacted]	[redacted]	8 µM
[redacted]	[redacted]	[redacted]	18 µM

Table 3. Name, catalogue number and working concentration of selective [redacted].

[redacted] antibody arrays

Proteome Profiler™ Mouse [redacted] Antibody Array (R&D Systems) was used to assay retinal lysates derived from PBS/NMDA-injected (24 hpi) and from WT/*rd10* (P18) mice. Manufacturer's recommendations were followed. Briefly, arrays were probed with a total of 200 µg proteins from retinal lysates. Membranes were developed by standard chemiluminescence techniques. Pixel intensity was quantified using the ImageJ software. The net level of each protein was calculated by the mean of the individual spot intensity minus the mean of the background intensity. Relative spot intensities are presented as mean ± SEM.

[redacted] constructs and [redacted]

Mouse [redacted] coding sequences (CDSs) were amplified by reverse transcribing total mouse spleen RNA (Superscript III RT Kit, Invitrogen) and then amplifying the full-length CDSs by PCR (using the Phusion hot start high fidelity polymerase, Thermofisher). The oligoes used are listed in Table 4. Resultant cDNA was C-terminally tagged with an HA and inserted into a lentiviral vector with a p1494 backbone, containing an EF1α promoter. An eGFP reporter was also present, with its expression being driven by a constitutive SV40 promoter [redacted] For the generation of the [redacted] double expressing [redacted] line, the constitutive eGFP reporter of the [redacted]

construct was replaced by a hygromycin resistance marker [redacted]

For [redacted] were produced following the RNA interference [redacted] constructs were FACS-sorted based on fluorescent intensity. Cells transduced with [redacted] were FACS-sorted based on fluorescent intensity and subjected to hygromycin selection (50 µg ml^{-1}) starting two days after the second round of [redacted]

Gene	Primer FW	Primer RV
[redacted]	[redacted]	[redacted]
[redacted]	[redacted]	[redacted]
[redacted]	[redacted]	[redacted]
[redacted]	[redacted]	[redacted]
[redacted]	[redacted]	[redacted]
[redacted]	[redacted]	[redacted]

Table 4. List of primers used to amplify [redacted] CDSs from total mouse spleen cDNA.

Immunofluorescence of [redacted] lines

[redacted] were plated into Lab-Tek chambers. The following day, they were washed (PBS), fixed (4% PFA, 10 min), permeabilized (0.2% Triton X-100 in PBS, 10 min) and blocked (3% BSA, 300 μM glycine, 0.02% Triton X-100 in PBS, 1h).

Incubation with primary antibodies lasted 3h (at RT). Cells were then washed with PBS and incubated with secondary antibodies (1.5h, at RT). DAPI (5mg ml^{-1}) was also used to stain for cell nuclei. Images were acquired using the Leica SP8 confocal microscope.

The following antibodies were used: chicken anti-GFP (1:200; ab13970, Abcam); mouse anti-HA (1:150; 11583816001, Roche); mouse anti-*βIII-tubulin (1:200; ab7751, Abcam);* anti-chicken Alexa Fluor 488; anti-mouse Alexa Fluor 568. All secondary antibodies

were provided by Molecular Probes (Invitrogen) and used 1:1'000 in PBS.

Flow cytometry analysis of [redacted] and retinal samples

For flow cytometry analysis, cultured [redacted] were detached with Accutase and collected by centrifugation at 300 rcf for 5 min. They were resuspended at a concentration of $1*10^6$ cells ml^{-1} and incubated with purified Rat Anti-Mouse CD16/CD32 (Mouse BD Fc Block™; BD Pharmingen™) at a concentration of 5 µg ml^{-1} (in PBS), 20 min at 4 °C. Following two washes in PBS, cells were incubated with conjugated primary antibodies (in PBS) for 30 min at 4 °C, in the dark. Finally, they were washed (PBS) and resuspended in PBS + DAPI (5mg ml^{-1}) for flow cytometry analysis. The following antibodies were used: PE anti-mouse [redacted]

All antibodies were purchased from R&D Systems and used at a concentration of 10µl/10^6cells.

For flow cytometry analysis of retinal samples, retinae were dissected from the enucleated eyes and incubated (30 min, 37 ºC) in trypsin supplemented with 0.1 mg ml^{-1} DNAseI for 20-30 minutes at 37ºC. Samples were then mechanically triturated, filtered, pelleted, and re-suspended in PBS for flow cytometry analysis. DAPI (5mg ml^{-1}) was also added to exclude dead cells from the analysis. Both NMDA-

damaged *rd10* eyes were analyzed 4 dpi.

Fixing, sectioning and immunofluorescence

Eyes were enucleated and fixed by immersion in 4% PFA overnight at 4°C; they were embedded in paraffin the following day. Serial transversal sections of 5µm of thickness were prepared and processed for immunofluorescence staining. Briefly, sections were de-paraffinized by sequential treatment with Xilene and EtOH gradient; slices were then placed in a plastic rack with a permeabilization buffer containing 0.3%Triton X-100 and 0.1M NaCitrate in PBS (1h at RT). Antigen retrieval was then performed by boiling the slides for 4 minutes in a domestic microwave. After a wash with cold water, sections were blocked for 1h (3% BSA, 300 µM glycine, 0.03% Triton X-100, 0.01M NaCitrate in PBS). They were then incubated overnight at 4ºC with primary antibodies diluted in PBS, 1.5% BSA. On the following day, slides were washed with PBS and incubated with secondary antibodies for 2h at room temperature.

For retinal flat mount immunostaining, whole retinae were dissected from previously fixed eye globes, and left an additional 30min in 4% PFA. They were then permeabilized (0.3% Triton X-100 in PBS, 1.5h at RT) and blocked for 1h at RT (3% BSA, 300 µM glycine, 0.03% Triton X-100, in PBS). Incubation with primary antibodies lasted two consecutive overnights at 4ºC. Retinae were then washed with PBS and incubated with secondary antibodies (overnight at 4ºC). DAPI (5mg ml^{-1}) was also used to stain for cell nuclei.

Following imaging, retinal flat mounts were embedded in paraffin, sectioned and processed for immunofluorescence re-staining as described for eye globes transversal sections.

The following antibodies were used: chicken anti-GFP (1:200; ab13970, Abcam); mouse anti-*βIII-tubulin (1:200; ab7751, Abcam);* anti-chicken Alexa Fluor 488, anti-mouse Alexa Fluor 568, anti-rabbit Alexa Fluor 568, anti-mouse Alexa Fluor 647 and anti-rabbit Alexa Fluor 633. All secondary antibodies were provided by Molecular Probes (Invitrogen) and used 1:1'000 in PBS. DAPI (5mg ml^{-1}) was used to stain for cell nuclei.

Both retinal flat mounts and sections were mounted with Vectashield (Vector Laboratories, 42 Burlingame, CA, USA) and imaged using either Leica laser SP5 or SP8 confocal microscopy systems.

Image processing and quantification

Images from both sections and whole retinal flat mounts were processed with the ImageJ software. Quantifications were based on analysis of at least three animals. We analyzed a minimum of ten sections per mouse, and three random fields per section. For each flat mount, we imaged at least three random fields.

To quantify the number of GFP^+ [redacted] differentiating into ganglion-amacrine neurons in flat mounts, GFP^+ total [redacted] and double positive $GFP^+/\beta III\text{-}tubulin^+$ cells were counted in at least ten sections

per animal (20X objective). The "transdifferentiation rate" was expressed as the percentage of the GFP^+/βIII-$tubulin^+$ cells over the total GFP^+ cells, ± SEM.

Statistical Analysis

As specified in the figure legends, data is presented as mean ± SEM or Min to Max boxes (with line at median). All statistical tests and graphs were generated using the Prism 8.0 software (GraphPad, San Diego, CA). Depending on the experimental setup, we used Mann-Whitney test, Two-tailed Student's T-test or One Way Anova. In all cases, a p value < 0.05 was considered significant (*, P <0.05; **, P <0.01; ***, P <0.001; ****, P <0.0001; ns, not significant).

BIBLIOGRAPHY

BIBLIOGRAPHY

1. W. Heavner, L. Pevny, Eye development and retinogenesis. *Cold Spring Harb Perspect Biol* **4**, (2012).
2. C. Cepko, Intrinsically different retinal progenitor cells produce specific types of progeny. *Nat Rev Neurosci* **15**, 615-627 (2014).
3. R. Wetts, S. E. Fraser, Multipotent precursors can give rise to all major cell types of the frog retina. *Science* **239**, 1142-1145 (1988).
4. C. J. Jeon, E. Strettoi, R. H. Masland, The major cell populations of the mouse retina. *J Neurosci* **18**, 8936-8946 (1998).
5. H. Wassle, H. J. Riemann, The mosaic of nerve cells in the mammalian retina. *Proc R Soc Lond B Biol Sci* **200**, 441-461 (1978).
6. A. Reichenbach, A. Bringmann, New functions of Muller cells. *Glia* **61**, 651-678 (2013).
7. A. Bringmann *et al.*, Role of retinal glial cells in neurotransmitter uptake and metabolism. *Neurochem Int* **54**, 143-160 (2009).
8. R. H. Masland, The Neuronal Organization of the Retina. *Neuron* **76**, 266-280 (2012).
9. X. Wang, A. Iannaccone, M. M. Jablonski, Contribution of Muller cells toward the regulation of photoreceptor outer segment assembly. *Neuron Glia Biol* **1**, 291-296 (2004).
10. F. Rieke, Mechanisms of single-photon detection in rod photoreceptors. *Methods Enzymol* **316**, 186-202 (2000).
11. R. R. A. Bourne *et al.*, Magnitude, temporal trends, and projections of the global prevalence of blindness and distance and near vision impairment: a systematic review and meta-analysis. *Lancet Glob Health* **5**, e888-e897 (2017).
12. C. Bunce, R. Wormald, Leading causes of certification for blindness and partial sight in England & Wales. *BMC Public Health* **6**, 58 (2006).
13. J. L. Haines *et al.*, Complement factor H variant increases the risk of age-related macular degeneration. *Science* **308**, 419-421 (2005).

14. A. J. Churchill *et al.*, VEGF polymorphisms are associated with neovascular age-related macular degeneration. *Human Molecular Genetics* **15**, 2955-2961 (2006).
15. R. D. Jager, W. F. Mieler, J. W. Miller, Age-related macular degeneration. *New England Journal of Medicine* **358**, (2008).
16. M. A. Genead, G. A. Fishman, E. M. Stone, R. Allikmets, The natural history of stargardt disease with specific sequence mutation in the ABCA4 gene. *Investigative Ophthalmology and Visual Science* **50**, 5867-5871 (2009).
17. P. P. Bither, L. A. Berns, Stargardt's disease: a review of the literature. *Journal of the American Optometric Association* **59**, 106-111 (1988).
18. D. T. Hartong, E. L. Berson, T. P. Dryja, Retinitis pigmentosa. *Lancet* **368**, 1795-1809 (2006).
19. F. Parmeggiani, Clinics, epidemiology and genetics of retinitis pigmentosa. *Current Genomics* **12**, 236-237 (2011).
20. R. K. Koenekoop, An overview of Leber congenital amaurosis: a model to understand human retinal development. *Surv Ophthalmol* **49**, 379-398 (2004).
21. J. Schuil, F. M. Meire, J. W. Delleman, Mental retardation in amaurosis congenita of Leber. *Neuropediatrics* **29**, 294-297 (1998).
22. I. Casteels *et al.*, Leber congenital amaurosis--differential diagnosis, ophthalmological and neuroradiological report of 18 patients. *Neuropediatrics* **27**, 189-193 (1996).
23. M. Jasiak-Zatonska, A. Kalinowska-Lyszczarz, S. Michalak, W. Kozubski, The immunology of neuromyelitis optica—Current knowledge, clinical implications, controversies and future perspectives. *International Journal of Molecular Sciences* **17**, (2016).
24. B. C. Chaon, M. S. Lee, Is there treatment for traumatic optic neuropathy? *Current Opinion in Ophthalmology* **26**, 445-449 (2015).
25. B. A. Sabel, J. Sautter, T. Stoehr, R. Siliprandi, A behavioral model of excitotoxicity: retinal degeneration, loss of vision, and subsequent recovery after intraocular NMDA administration in adult rats. *Exp Brain Res* **106**, 93-105 (1995).
26. D. R. Lucas, J. P. Newhouse, The toxic effect of sodium L-glutamate on the inner layers of the retina. *AMA Arch Ophthalmol* **58**, 193-201 (1957).

27. R. Siliprandi *et al.*, N-methyl-D-aspartate-induced neurotoxicity in the adult rat retina. *Vis Neurosci* **8**, 567-573 (1992).
28. N. J. Sucher, S. A. Lipton, E. B. Dreyer, Molecular basis of glutamate toxicity in retinal ganglion cells. *Vision Res* **37**, 3483-3493 (1997).
29. B. Chang *et al.*, Retinal degeneration mutants in the mouse. *Vision Res* **42**, 517-525 (2002).
30. B. Chang *et al.*, Two mouse retinal degenerations caused by missense mutations in the beta-subunit of rod cGMP phosphodiesterase gene. *Vision Res* **47**, 624-633 (2007).
31. C. Martínez-Fernández de la Cámara *et al.*, Adalimumab Reduces Photoreceptor Cell Death in A Mouse Model of Retinal Degeneration. *Sci Rep* **5**, (2015).
32. P. A. Newmark, A. Sanchez Alvarado, Bromodeoxyuridine specifically labels the regenerative stem cells of planarians. *Developmental biology* **220**, 142-153 (2000).
33. A. Kumar, C. P. Velloso, Y. Imokawa, J. P. Brockes, Plasticity of retrovirus-labelled myotubes in the newt limb regeneration blastema. *Developmental biology* **218**, 125-136 (2000).
34. L. Spallanzani, *An Essay on Animal Reproductions.*, (T Becket, London (translated from Italian by M. Maty), 1769).
35. J. P. Brockes, A. Kumar, Plasticity and reprogramming of differentiated cells in amphibian regeneration. *Nature reviews. Molecular cell biology* **3**, 566-574 (2002).
36. K. D. Poss, L. G. Wilson, M. T. Keating, Heart regeneration in zebrafish. *Science (New York, N.Y.)* **298**, 2188-2190 (2002).
37. A. Raya *et al.*, Activation of Notch signaling pathway precedes heart regeneration in zebrafish. *Proceedings of the National Academy of Sciences of the United States of America* **100 Suppl 1**, 11889-11895 (2003).
38. Z. L. Chen, W. M. Yu, S. Strickland, Peripheral regeneration. *Annual review of neuroscience* **30**, 209-233 (2007).
39. M. Pesaresi, R. Sebastian-Perez, M. P. Cosma, Dedifferentiation, transdifferentiation and cell fusion: in vivo reprogramming strategies for regenerative medicine. *Febs j*, (2018).
40. V. L. Colucci, Sulla rigenerazione parziale dell'occhio nei Tritoni- Istogenesi e sviluppo. Studio sperimentale. *Mem. R. Acad. Sci. Ist. Bologna*, 593–629 (1891).

41. D. Goldman, Muller glial cell reprogramming and retina regeneration. *Nat Rev Neurosci* **15**, 431-442 (2014).
42. A. J. Fischer, T. A. Reh, Potential of Muller glia to become neurogenic retinal progenitor cells. *Glia* **43**, 70-76 (2003).
43. D. T. Scadden, The stem-cell niche as an entity of action. *Nature* **441**, 1075-1079 (2006).
44. C. S. Potten, M. Loeffler, Stem cells: attributes, cycles, spirals, pitfalls and uncertainties. Lessons for and from the crypt. *Development (Cambridge, England)* **110**, 1001-1020 (1990).
45. C. Blanpain, W. E. Lowry, A. Geoghegan, L. Polak, E. Fuchs, Self-renewal, multipotency, and the existence of two cell populations within an epithelial stem cell niche. *Cell* **118**, 635-648 (2004).
46. E. K. Nishimura *et al.*, Dominant role of the niche in melanocyte stem-cell fate determination. *Nature* **416**, 854-860 (2002).
47. K. A. Moore, I. R. Lemischka, Stem cells and their niches. *Science* **311**, 1880-1885 (2006).
48. J. Pellettieri, A. Sanchez Alvarado, Cell turnover and adult tissue homeostasis: from humans to planarians. *Annu Rev Genet* **41**, 83-105 (2007).
49. O. Bergmann *et al.*, Evidence for cardiomyocyte renewal in humans. *Science* **324**, 98-102 (2009).
50. O. Bergmann, S. Jovinge, Cardiac regeneration in vivo: mending the heart from within? *Stem Cell Res* **13**, 523-531 (2014).
51. T. H. Cheung, T. A. Rando, Molecular regulation of stem cell quiescence. *Nat Rev Mol Cell Biol* **14**, 329-340 (2013).
52. D. E. Cohen, D. Melton, Turning straw into gold: directing cell fate for regenerative medicine. *Nature reviews. Genetics* **12**, 243-252 (2011).
53. L. Qian *et al.*, In vivo reprogramming of murine cardiac fibroblasts into induced cardiomyocytes. *Nature* **485**, 593-598 (2012).
54. K. Song *et al.*, Heart repair by reprogramming non-myocytes with cardiac transcription factors. *Nature* **485**, 599-604 (2012).
55. N. Kapoor, W. Liang, E. Marban, H. C. Cho, Direct conversion of quiescent cardiomyocytes to pacemaker cells by expression of Tbx18. *Nature biotechnology* **31**, 54-62 (2013).

56. M. Pesaresi, S. A. Bonilla-Pons, M. P. Cosma, In vivo somatic cell reprogramming for tissue regeneration: the emerging role of the local microenvironment. *Curr Opin Cell Biol* **55**, 119-128 (2018).
57. F. W. Pagliuca *et al.*, Generation of functional human pancreatic beta cells in vitro. *Cell* **159**, 428-439 (2014).
58. A. Rezania *et al.*, Reversal of diabetes with insulin-producing cells derived in vitro from human pluripotent stem cells. *Nature biotechnology* **32**, 1121-1133 (2014).
59. R. L. Bernardos, L. K. Barthel, J. R. Meyers, P. A. Raymond, Late-stage neuronal progenitors in the retina are radial Muller glia that function as retinal stem cells. *J Neurosci* **27**, 7028-7040 (2007).
60. J. R. Lenkowski, P. A. Raymond, Muller glia: Stem cells for generation and regeneration of retinal neurons in teleost fish. *Prog Retin Eye Res* **40**, 94-123 (2014).
61. M. Nagashima, L. K. Barthel, P. A. Raymond, A self-renewing division of zebrafish Muller glial cells generates neuronal progenitors that require N-cadherin to regenerate retinal neurons. *Development* **140**, 4510-4521 (2013).
62. R. Thummel *et al.*, Characterization of Muller glia and neuronal progenitors during adult zebrafish retinal regeneration. *Exp Eye Res* **87**, 433-444 (2008).
63. A. J. Fischer, T. A. Reh, Muller glia are a potential source of neural regeneration in the postnatal chicken retina. *Nat Neurosci* **4**, 247-252 (2001).
64. D. Gallina, I. Palazzo, L. Steffenson, L. Todd, A. J. Fischer, Wnt/beta-catenin-signaling and the formation of Muller glia-derived progenitors in the chick retina. *Dev Neurobiol* **76**, 983-1002 (2016).
65. M. O. Karl *et al.*, Stimulation of neural regeneration in the mouse retina. *Proc Natl Acad Sci U S A* **105**, 19508-19513 (2008).
66. J. Wan *et al.*, Preferential regeneration of photoreceptor from Muller glia after retinal degeneration in adult rat. *Vision Res* **48**, 223-234 (2008).
67. S. Ooto *et al.*, Potential for neural regeneration after neurotoxic injury in the adult mammalian retina. *Proc Natl Acad Sci U S A* **101**, 13654-13659 (2004).
68. L. Todd, L. I. Volkov, C. Zelinka, N. Squires, A. J. Fischer, Heparin-binding EGF-like growth factor (HB-EGF) stimulates the

proliferation of Muller glia-derived progenitor cells in avian and murine retinas. *Mol Cell Neurosci* **69**, 54-64 (2015).
69. M. Pesaresi *et al.*, Endogenous Mobilization of Bone-Marrow Cells Into the Murine Retina Induces Fusion-Mediated Reprogramming of Muller Glia Cells. *EBioMedicine*, (2018).
70. M. K. Webster *et al.*, Evidence of BrdU-positive retinal neurons after application of an Alpha7 nicotinic acetylcholine receptor agonist. *Neuroscience* **346**, 437-446 (2017).
71. D. Sanges *et al.*, Wnt/beta-catenin signaling triggers neuron reprogramming and regeneration in the mouse retina. *Cell Rep* **4**, 271-286 (2013).
72. D. Sanges *et al.*, Reprogramming Muller glia via in vivo cell fusion regenerates murine photoreceptors. *J Clin Invest* **126**, 3104-3116 (2016).
73. M. O. Karl, T. A. Reh, Regenerative medicine for retinal diseases: activating endogenous repair mechanisms. *Trends Mol Med* **16**, 193-202 (2010).
74. J. Pollak *et al.*, ASCL1 reprograms mouse Muller glia into neurogenic retinal progenitors. *Development* **140**, 2619-2631 (2013).
75. Y. Ueki *et al.*, Transgenic expression of the proneural transcription factor Ascl1 in Muller glia stimulates retinal regeneration in young mice. *Proc Natl Acad Sci U S A* **112**, 13717-13722 (2015).
76. N. L. Jorstad *et al.*, Stimulation of functional neuronal regeneration from Muller glia in adult mice. *Nature* **548**, 103-107 (2017).
77. F. Osakada *et al.*, Wnt signaling promotes regeneration in the retina of adult mammals. *J Neurosci* **27**, 4210-4219 (2007).
78. J. L. Close, J. Liu, B. Gumuscu, T. A. Reh, Epidermal growth factor receptor expression regulates proliferation in the postnatal rat retina. *Glia* **54**, 94-104 (2006).
79. Z. Tao *et al.*, Lin28B promotes Muller glial cell de-differentiation and proliferation in the regenerative rat retinas. *Oncotarget* **7**, 49368-49383 (2016).
80. K. Yao *et al.*, Wnt Regulates Proliferation and Neurogenic Potential of Muller Glial Cells via a Lin28/let-7 miRNA-Dependent Pathway in Adult Mammalian Retinas. *Cell Rep* **17**, 165-178 (2016).

81. B. A. Tucker *et al.*, Transplantation of adult mouse iPS cell-derived photoreceptor precursors restores retinal structure and function in degenerative mice. *PLoS ONE* **6**, (2011).
82. M. D. Tibbetts, M. A. Samuel, T. S. Chang, A. C. Ho, Stem cell therapy for retinal disease. *Curr Opin Ophthalmol* **23**, 226-234 (2012).
83. D. Merino, P. Loza-Alvarez, Adaptive optics scanning laser ophthalmoscope imaging: Technology update. *Clinical Ophthalmology* **10**, 743-755 (2016).
84. D. Scoles *et al.*, Assessing photoreceptor structure associated with ellipsoid zone disruptions visualized with optical coherence tomography. *Retina* **36**, 91-103 (2016).
85. M. A. Zarbin, R. P. Casaroli-Marano, P. J. Rosenfeld, in *Cell-Based Therapy for Retinal Degenerative Disease*. (2014), vol. 53, pp. 1-32.
86. M. Menghini, J. L. Duncan, in *Developments in Ophthalmology*. (2014), vol. 53, pp. 53-69.
87. S. Zayit-Soudry, J. L. Duncan, R. Syed, M. Menghini, A. J. Roorda, Cone structure imaged with adaptive optics scanning laser ophthalmoscopy in eyes with nonneovascular age-related macular degeneration. *Investigative Ophthalmology and Visual Science* **54**, 7498-7509 (2013).
88. V. L. Perez, A. M. Saeed, Y. Tan, M. Urbieta, F. Cruz-Guilloty, The eye: A window to the soul of the immune system. *J Autoimmun* **45**, 7-14 (2013).
89. P. Zamiri, S. Sugita, J. W. Streilein, in *Chemical Immunology and Allergy*. (2007), vol. 92, pp. 86-93.
90. J. W. Streilein, Ocular immune privilege: The eye takes a dim but practical view of immunity and inflammation. *Journal of Leukocyte Biology* **74**, 179-185 (2003).
91. R. D. Lund *et al.*, Cells isolated from umbilical cord tissue rescue photoreceptors and visual functions in a rodent model of retinal disease. *Stem Cells* **25**, 602-611 (2007).
92. Y. Inoue *et al.*, Subretinal transplantation of bone marrow mesenchymal stem cells delays retinal degeneration in the RCS rat model of retinal degeneration. *Exp Eye Res* **85**, 234-241 (2007).
93. A. Tzameret *et al.*, Transplantation of human bone marrow mesenchymal stem cells as a thin subretinal layer

ameliorates retinal degeneration in a rat model of retinal dystrophy. *Experimental Eye Research* **118**, 135-144 (2014).
94. Y. Zhang, W. Wang, Effects of bone marrow mesenchymal stem cell transplantation on light-damaged retina. *Invest Ophthalmol Vis Sci* **51**, 3742-3748 (2010).
95. S. Arnhold, Y. Absenger, H. Klein, K. Addicks, U. Schraermeyer, Transplantation of bone marrow-derived mesenchymal stem cells rescue photoreceptor cells in the dystrophic retina of the rhodopsin knockout mouse. *Graefe's Archive for Clinical and Experimental Ophthalmology* **245**, 414-422 (2007).
96. T. V. Johnson *et al.*, Neuroprotective effects of intravitreal mesenchymal stem cell transplantation in experimental glaucoma. *Investigative Ophthalmology and Visual Science* **51**, 2051-2059 (2010).
97. S. Yu, T. Tanabe, M. Dezawa, H. Ishikawa, N. Yoshimura, Effects of bone marrow stromal cell injection in an experimental glaucoma model. *Biochemical and Biophysical Research Communications* **344**, 1071-1079 (2006).
98. H. Levkovitch-Verbin *et al.*, Intravitreal injections of neurotrophic factors secreting mesenchymal stem cells are neuroprotective in rat eyes following optic nerve transaction. *Investigative Ophthalmology and Visual Science* **51**, 6394-6400 (2010).
99. B. Mead, A. Logan, M. Berry, W. Leadbeater, B. A. Scheven, Intravitreally transplanted dental pulp stem cells promote neuroprotection and axon regeneration of retinal ganglion cells after optic nerve injury. *Invest Ophthalmol Vis Sci* **54**, 7544-7556 (2013).
100. B. Lu *et al.*, Human adult bone marrow-derived somatic cells rescue vision in a rodent model of retinal degeneration. *Experimental Eye Research* **91**, 449-455 (2010).
101. A. Otani *et al.*, Rescue of retinal degeneration by intravitreally injected adult bone marrow-derived lineage-negative hematopoietic stem cells. *Journal of Clinical Investigation* **114**, 765-774 (2004).
102. D. Sanges *et al.*, Reprogramming Muller glia via in vivo cell fusion regenerates murine photoreceptors. *J Clin Invest*, (2016).
103. H. C. Wang, J. Brown, H. Alayon, B. E. Stuck, Transplantation of quantum dot-labelled bone marrow-derived

stem cells into the vitreous of mice with laser-induced retinal injury: survival, integration and differentiation. *Vision Res* **50**, 665-673 (2010).
104. S. S. Park *et al.*, Long-term effects of intravitreal injection of GMP-grade bone-marrow-derived CD34+ cells in NOD-SCID mice with acute ischemia-reperfusion injury. *Invest Ophthalmol Vis Sci* **53**, 986-994 (2012).
105. B. Lu *et al.*, Long-term safety and function of RPE from human embryonic stem cells in preclinical models of macular degeneration. *Stem Cells* **27**, 2126-2135 (2009).
106. R. D. Lund *et al.*, Human embryonic stem cell-derived cells rescue visual function in dystrophic RCS rats. *Cloning Stem Cells* **8**, 189-199 (2006).
107. A. J. Carr *et al.*, Protective effects of human iPS-derived retinal pigment epithelium cell transplantation in the retinal dystrophic rat. *PLoS ONE* **4**, (2009).
108. A. Vugler *et al.*, Elucidating the phenomenon of HESC-derived RPE: Anatomy of cell genesis, expansion and retinal transplantation. *Experimental Neurology* **214**, 347-361 (2008).
109. S. Wang *et al.*, Morphological and functional rescue in RCS rats after RPE cell line transplantation at a later stage of degeneration. *Invest Ophthalmol Vis Sci* **49**, 416-421 (2008).
110. D. M. Gamm *et al.*, Protection of visual functions by human neural progenitors in a rat model of retinal disease. *PLoS One* **2**, e338 (2007).
111. S. Wang *et al.*, Long-term vision rescue by human neural progenitors in a rat model of photoreceptor degeneration. *Invest Ophthalmol Vis Sci* **49**, 3201-3206 (2008).
112. T. J. McGill *et al.*, Transplantation of human central nervous system stem cells - neuroprotection in retinal degeneration. *European Journal of Neuroscience* **35**, 468-477 (2012).
113. J. S. Meyer, M. L. Katz, J. A. Maruniak, M. D. Kirk, Embryonic stem cell-derived neural progenitors incorporate into degenerating retina and enhance survival of host photoreceptors. *Stem Cells* **24**, 274-283 (2006).
114. G. Jung *et al.*, Genetically modified neural stem cells for a local and sustained delivery of neuroprotective factors to the dystrophic mouse retina. *Stem Cells Translational Medicine* **2**, 1001-1010 (2013).

115. A. Nishida *et al.*, Incorporation and differentiation of hippocampus-derived neural stem cells transplanted in injured adult rat retina. *Investigative Ophthalmology and Visual Science* **41**, 4268-4274 (2000).
116. S. D. Grozdanic *et al.*, Morphological integration and functional assessment of transplanted neural progenitor cells in healthy and acute ischemic rat eyes. *Experimental Eye Research* **82**, 597-607 (2006).
117. H. J. Klassen *et al.*, Multipotent retinal progenitors express developmental markers, differentiate into retinal neurons, and preserve light-mediated behavior. *Investigative Ophthalmology and Visual Science* **45**, 4167-4173 (2004).
118. G. Qiu *et al.*, Photoreceptor differentiation and integration of retinal progenitor cells transplanted into transgenic rats. *Experimental Eye Research* **80**, 515-525 (2005).
119. R. A. Pearson *et al.*, Restoration of vision after transplantation of photoreceptors. *Nature* **485**, 99-103 (2012).
120. S. Singhal *et al.*, Human müller glia with stem cell characteristics differentiate into retinal ganglion cell (RGC) precursors in vitro and partially restore RGC function in vivo following transplantation. *Stem Cells Translational Medicine* **1**, 188-199 (2012).
121. P. M. Sottile F., Simonte G., Cosma M.P., in *Cell-based therapy for degenerative retinal disease,* S. M. Zarbin M., Casaroli-Marano R. , Ed. (Humana Press, Cham, 2019), chap. 12, pp. pp 217-244.
122. K. H. Niederkorn JY, *Immune response and the eye*. 2nd Revised ed. Basel (Karger, 2007).
123. S. Sugita, Y. Futagami, S. B. Smith, H. Naggar, M. Mochizuki, Retinal and ciliary body pigment epithelium suppress activation of T lymphocytes via transforming growth factor beta. *Experimental Eye Research* **83**, 1459-1471 (2006).
124. T. A. Ferguson, T. S. Griffith, in *Chemical Immunology and Allergy*. (2007), vol. 92, pp. 140-154.
125. S. Sugita *et al.*, Retinal pigment epithelium-derived CTLA-2alpha induces TGFbeta-producing T regulatory cells. *Journal of immunology (Baltimore, Md. : 1950)* **181**, 7525-7536 (2008).
126. J. H. Sohn, H. J. Kaplan, H. J. Suk, P. S. Bora, N. S. Bora, Chronic low level complement activation within the eye is

controlled by intraocular complement regulatory proteins. *Invest Ophthalmol Vis Sci* **41**, 3492-3502 (2000).
127. N. S. Bora, C. L. Gobleman, J. P. Atkinson, J. S. Pepose, H. J. Kaplan, Differential expression of the complement regulatory proteins in the human eye. *Invest Ophthalmol Vis Sci* **34**, 3579-3584 (1993).
128. B. W. McBride, J. I. McGill, J. L. Smith, MHC class I and class II antigen expression in normal human corneas and in corneas from cases of herpetic keratitis. *Immunology* **65**, 583-587 (1988).
129. M. J. Evans, M. H. Kaufman, Establishment in culture of pluripotential cells from mouse embryos. *Nature* **292**, 154-156 (1981).
130. G. R. Martin, Isolation of a pluripotent cell line from early mouse embryos cultured in medium conditioned by teratocarcinoma stem cells. *Proc Natl Acad Sci U S A* **78**, 7634-7638 (1981).
131. C. E. Murry, G. Keller, Differentiation of embryonic stem cells to clinically relevant populations: lessons from embryonic development. *Cell* **132**, 661-680 (2008).
132. K. Takahashi, S. Yamanaka, Induction of pluripotent stem cells from mouse embryonic and adult fibroblast cultures by defined factors. *Cell* **126**, 663-676 (2006).
133. K. Takahashi *et al.*, Induction of pluripotent stem cells from adult human fibroblasts by defined factors. *Cell* **131**, 861-872 (2007).
134. J. Yu *et al.*, Induced pluripotent stem cell lines derived from human somatic cells. *Science (New York, N.Y.)* **318**, 1917-1920 (2007).
135. I. H. Park *et al.*, Reprogramming of human somatic cells to pluripotency with defined factors. *Nature* **451**, 141-146 (2008).
136. J. Hanna *et al.*, Treatment of sickle cell anemia mouse model with iPS cells generated from autologous skin. *Science (New York, N.Y.)* **318**, 1920-1923 (2007).
137. M. Wernig *et al.*, Neurons derived from reprogrammed fibroblasts functionally integrate into the fetal brain and improve symptoms of rats with Parkinson's disease. *Proceedings of the National Academy of Sciences of the United States of America* **105**, 5856-5861 (2008).
138. Z. Alipio *et al.*, Reversal of hyperglycemia in diabetic mouse models using induced-pluripotent stem (iPS)-derived

pancreatic beta-like cells. *Proceedings of the National Academy of Sciences of the United States of America* **107**, 13426-13431 (2010).
139. O. Tsuji *et al.*, Therapeutic potential of appropriately evaluated safe-induced pluripotent stem cells for spinal cord injury. *Proceedings of the National Academy of Sciences of the United States of America* **107**, 12704-12709 (2010).
140. B. Lu, C. W. Morgans, S. Girman, R. Lund, S. Wang, Retinal morphological and functional changes in an animal model of retinitis pigmentosa. *Vis Neurosci* **30**, 77-89 (2013).
141. A. Gonzalez-Cordero *et al.*, Photoreceptor precursors derived from three-dimensional embryonic stem cell cultures integrate and mature within adult degenerate retina. *Nat Biotechnol* **31**, 741-747 (2013).
142. S. Decembrini, U. Koch, F. Radtke, A. Moulin, Y. Arsenijevic, Derivation of traceable and transplantable photoreceptors from mouse embryonic stem cells. *Stem Cell Reports* **2**, 853-865 (2014).
143. S. Wang *et al.*, Long-term vision rescue by human neural progenitors in a rat model of photoreceptor degeneration. *Investigative Ophthalmology and Visual Science* **49**, 3201-3206 (2008).
144. N. Cuenca *et al.*, Phagocytosis of photoreceptor outer segments by transplanted human neural stem cells as a neuroprotective mechanism in retinal degeneration. *Investigative Ophthalmology and Visual Science* **54**, 6745-6756 (2013).
145. C. B. Mellough *et al.*, Fate of multipotent neural precursor cells transplanted into mouse retina selectively depleted of retinal ganglion cells. *Experimental Neurology* **186**, 6-19 (2004).
146. D. A. Lamba, M. O. Karl, C. B. Ware, T. A. Reh, Efficient generation of retinal progenitor cells from human embryonic stem cells. *Proc Natl Acad Sci U S A* **103**, 12769-12774 (2006).
147. K. Homma *et al.*, Developing rods transplanted into the degenerating retina of Crx-knockout mice exhibit neural activity similar to native photoreceptors. *Stem Cells* **31**, 1149-1159 (2013).
148. M. S. Singh *et al.*, Reversal of end-stage retinal degeneration and restoration of visual function by photoreceptor transplantation. *Proc Natl Acad Sci U S A* **110**, 1101-1106 (2013).

149. E. L. West *et al.*, Defining the integration capacity of embryonic stem cell-derived photoreceptor precursors. *Stem Cells* **30**, 1424-1435 (2012).
150. E. Banin *et al.*, Retinal incorporation and differentiation of neural precursors derived from human embryonic stem cells. *Stem Cells* **24**, 246-257 (2006).
151. A. O. Cramer, R. E. MacLaren, Translating induced pluripotent stem cells from bench to bedside: application to retinal diseases. *Curr Gene Ther* **13**, 139-151 (2013).
152. S. Arnhold, H. Klein, I. Semkova, K. Addicks, U. Schraermeyer, Neurally selected embryonic stem cells induce tumor formation after long-term survival following engraftment into the subretinal space. *Investigative Ophthalmology and Visual Science* **45**, 4251-4255 (2004).
153. S. D. Schwartz *et al.*, Human embryonic stem cell-derived retinal pigment epithelium in patients with age-related macular degeneration and Stargardt's macular dystrophy: follow-up of two open-label phase 1/2 studies. *Lancet* **385**, 509-516 (2015).
154. S. D. Schwartz, G. Tan, H. Hosseini, A. Nagiel, Subretinal Transplantation of Embryonic Stem Cell-Derived Retinal Pigment Epithelium for the Treatment of Macular Degeneration: An Assessment at 4 Years. *Invest Ophthalmol Vis Sci* **57**, ORSFc1-9 (2016).
155. A. S. Berger, T. H. Tezel, L. V. Del Priore, H. J. Kaplan, Photoreceptor transplantation in retinitis pigmentosa: short-term follow-up. *Ophthalmology* **110**, 383-391 (2003).
156. H. J. Kaplan, T. H. Tezel, A. S. Berger, M. L. Wolf, L. V. Del Priore, Human photoreceptor transplantation in retinitis pigmentosa. A safety study. *Arch Ophthalmol* **115**, 1168-1172 (1997).
157. P. Gouras *et al.*, Survival and synapse formation of transplanted rat rods. *J Neural Transplant Plast* **2**, 91-100 (1991).
158. M. del Cerro, J. R. Ison, G. P. Bowen, E. Lazar, C. del Cerro, Intraretinal grafting restores visual function in light-blinded rats. *Neuroreport* **2**, 529-532 (1991).
159. K. English, K. J. Wood, Immunogenicity of embryonic stem cell-derived progenitors after transplantation. *Curr Opin Organ Transplant* **16**, 90-95 (2011).

160. R. Araki *et al.*, Negligible immunogenicity of terminally differentiated cells derived from induced pluripotent or embryonic stem cells. *Nature* **494**, 100-104 (2013).
161. S. Sugita *et al.*, Successful Transplantation of Retinal Pigment Epithelial Cells from MHC Homozygote iPSCs in MHC-Matched Models. *Stem Cell Reports* **7**, 635-648 (2016).
162. T. Zhao, Z. N. Zhang, Z. Rong, Y. Xu, Immunogenicity of induced pluripotent stem cells. *Nature* **474**, 212-216 (2011).
163. P. J. Fairchild, The challenge of immunogenicity in the quest for induced pluripotency. *Nature Reviews Immunology* **10**, 868-875 (2010).
164. S. Solomon, F. Pitossi, M. S. Rao, Banking on iPSC--is it doable and is it worthwhile. *Stem Cell Rev* **11**, 1-10 (2015).
165. M. Nakagawa *et al.*, Generation of induced pluripotent stem cells without Myc from mouse and human fibroblasts. *Nature Biotechnology* **26**, 101-106 (2008).
166. S. Zhu *et al.*, Reprogramming of human primary somatic cells by OCT4 and chemical compounds. *Cell Stem Cell* **7**, 651-655 (2010).
167. D. Huangfu *et al.*, Induction of pluripotent stem cells from primary human fibroblasts with only Oct4 and Sox2. *Nature Biotechnology* **26**, 1269-1275 (2008).
168. Y. Shi *et al.*, Induction of Pluripotent Stem Cells from Mouse Embryonic Fibroblasts by Oct4 and Klf4 with Small-Molecule Compounds. *Cell Stem Cell* **3**, 568-574 (2008).
169. K. Okita, M. Nakagawa, H. Hyenjong, T. Ichisaka, S. Yamanaka, Generation of mouse induced pluripotent stem cells without viral vectors. *Science* **322**, 949-953 (2008).
170. K. Kaji *et al.*, Virus-free induction of pluripotency and subsequent excision of reprogramming factors. *Nature* **458**, 771-775 (2009).
171. L. Warren *et al.*, Highly efficient reprogramming to pluripotency and directed differentiation of human cells with synthetic modified mRNA. *Cell Stem Cell* **7**, 618-630 (2010).
172. D. Kim *et al.*, Generation of Human Induced Pluripotent Stem Cells by Direct Delivery of Reprogramming Proteins. *Cell Stem Cell* **4**, 472-476 (2009).
173. A. Doi *et al.*, Differential methylation of tissue-and cancer-specific CpG island shores distinguishes human induced

pluripotent stem cells, embryonic stem cells and fibroblasts. *Nature Genetics* **41**, 1350-1353 (2009).
174. J. L. Liao *et al.*, Molecular signature of primary retinal pigment epithelium and stem-cell-derived RPE cells. *Human Molecular Genetics* **19**, 4229-4238 (2010).
175. H. Klassen, Stem cells in clinical trials for treatment of retinal degeneration. *Expert Opin Biol Ther* **16**, 7-14 (2016).
176. J. Hanus, F. Zhao, S. Wang, Current therapeutic developments in atrophic age-related macular degeneration. *Br J Ophthalmol* **100**, 122-127 (2016).
177. N. Serakinci, W. N. Keith, Therapeutic potential of adult stem cells. *Eur J Cancer* **42**, 1243-1246 (2006).
178. A. J. Merrell, B. Z. Stanger, Adult cell plasticity in vivo: de-differentiation and transdifferentiation are back in style. *Nat Rev Mol Cell Biol* **17**, 413-425 (2016).
179. B. G. Ballios, L. Clarke, B. L. K. Coles, M. S. Shoichet, D. Van Der Kooy, The adult retinal stem cell is a rare cell in the ciliary epithelium whose progeny can differentiate into photoreceptors. *Biology Open* **1**, 237-246 (2012).
180. I. Ahmad, L. Tang, H. Pham, Identification of neural progenitors in the adult mammalian eye. *Biochemical and Biophysical Research Communications* **270**, 517-521 (2000).
181. V. Tropepe *et al.*, Retinal stem cells in the adult mammalian eye. *Science* **287**, 2032-2036 (2000).
182. R. E. MacLaren *et al.*, Retinal repair by transplantation of photoreceptor precursors. *Nature* **444**, 203-207 (2006).
183. M. S. Humayun *et al.*, Human neural retinal transplantation. *Investigative Ophthalmology and Visual Science* **41**, 3100-3106 (2000).
184. M. S. Humayun *et al.*, Human neural retinal transplantation. *Invest Ophthalmol Vis Sci* **41**, 3100-3106 (2000).
185. R. A. Pearson *et al.*, Restoration of vision after transplantation of photoreceptors. *Nature* **485**, 99-103 (2012).
186. N. D. Radtke, R. B. Aramant, M. J. Seiler, H. M. Petry, D. Pidwell, Vision change after sheet transplant of fetal retina with retinal pigment epithelium to a patient with retinitis pigmentosa. *Arch Ophthalmol* **122**, 1159-1165 (2004).
187. B. L. K. Coles *et al.*, Facile isolation and the characterization of human retinal stem cells. *Proceedings of the*

National Academy of Sciences of the United States of America **101**, 15772-15777 (2004).
188. G. Ferrari *et al.*, Muscle regeneration by bone marrow-derived myogenic progenitors. *Science* **279**, 1528-1530 (1998).
189. K. A. Jackson *et al.*, Regeneration of ischemic cardiac muscle and vascular endothelium by adult stem cells. *J Clin Invest* **107**, 1395-1402 (2001).
190. D. Orlic *et al.*, Bone marrow cells regenerate infarcted myocardium. *Nature* **410**, 701-705 (2001).
191. B. E. Petersen *et al.*, Bone marrow as a potential source of hepatic oval cells. *Science* **284**, 1168-1170 (1999).
192. E. Lagasse *et al.*, Purified hematopoietic stem cells can differentiate into hepatocytes in vivo. *Nat Med* **6**, 1229-1234 (2000).
193. T. R. Brazelton, F. M. Rossi, G. I. Keshet, H. M. Blau, From marrow to brain: expression of neuronal phenotypes in adult mice. *Science* **290**, 1775-1779 (2000).
194. E. Mezey, K. J. Chandross, G. Harta, R. A. Maki, S. R. McKercher, Turning blood into brain: cells bearing neuronal antigens generated in vivo from bone marrow. *Science* **290**, 1779-1782 (2000).
195. J. Priller *et al.*, Neogenesis of cerebellar Purkinje neurons from gene-marked bone marrow cells in vivo. *J Cell Biol* **155**, 733-738 (2001).
196. A. Otani *et al.*, Rescue of retinal degeneration by intravitreally injected adult bone marrow-derived lineage-negative hematopoietic stem cells. *J Clin Invest* **114**, 765-774 (2004).
197. A. Tzameret *et al.*, Epiretinal transplantation of human bone marrow mesenchymal stem cells rescues retinal and vision function in a rat model of retinal degeneration. *Stem Cell Res* **15**, 387-394 (2015).
198. S. Arnhold *et al.*, Adenovirally transduced bone marrow stromal cells differentiate into pigment epithelial cells and induce rescue effects in RCS rats. *Invest Ophthalmol Vis Sci* **47**, 4121-4129 (2006).
199. R. Greco *et al.*, Allogeneic hematopoietic stem cell transplantation for neuromyelitis optica. *Annals of Neurology* **75**, 447-453 (2014).

200. C. A. Gregory, D. J. Prockop, J. L. Spees, Non-hematopoietic bone marrow stem cells: Molecular control of expansion and differentiation. *Experimental Cell Research* **306**, 330-335 (2005).
201. M. Dezawa *et al.*, Specific induction of neuronal cells from bone marrow stromal cells and application for autologous transplantation. *Journal of Clinical Investigation* **113**, 1701-1710 (2004).
202. A. Kicic *et al.*, Differentiation of marrow stromal cells into photoreceptors in the rat eye. *Journal of Neuroscience* **23**, 7742-7749 (2003).
203. M. F. Pittenger *et al.*, Multilineage potential of adult human mesenchymal stem cells. *Science* **284**, 143-147 (1999).
204. D. J. Prockop, Marrow stromal cells as stem cells for nonhematopoietic tissues. *Science* **276**, 71-74 (1997).
205. S. Mendez-Ferrer *et al.*, Mesenchymal and haematopoietic stem cells form a unique bone marrow niche. *Nature* **466**, 829-834 (2010).
206. M. Dominici *et al.*, Minimal criteria for defining multipotent mesenchymal stromal cells. The International Society for Cellular Therapy position statement. *Cytotherapy* **8**, 315-317 (2006).
207. N. G. Singer, A. I. Caplan, in *Annual Review of Pathology: Mechanisms of Disease*. (2011), vol. 6, pp. 457-478.
208. T. V. Johnson, N. D. Bull, K. R. Martin, Transplantation prospects for the inner retina. *Eye* **23**, 1980-1984 (2009).
209. D. I. Cho *et al.*, Mesenchymal stem cells reciprocally regulate the M1/M2 balance in mouse bone marrow-derived macrophages. *Exp Mol Med* **46**, e70 (2014).
210. S. Beyth *et al.*, Human mesenchymal stem cells alter antigen-presenting cell maturation and induce T-cell unresponsiveness. *Blood* **105**, 2214-2219 (2005).
211. M. E. Groh, B. Maitra, E. Szekely, O. N. Koc, Human mesenchymal stem cells require monocyte-mediated activation to suppress alloreactive T cells. *Exp Hematol* **33**, 928-934 (2005).
212. K. Le Blanc, L. Tammik, B. Sundberg, S. E. Haynesworth, O. Ringden, Mesenchymal stem cells inhibit and stimulate mixed lymphocyte cultures and mitogenic responses independently of the major histocompatibility complex. *Scand J Immunol* **57**, 11-20 (2003).

213. M. Di Nicola *et al.*, Human bone marrow stromal cells suppress T-lymphocyte proliferation induced by cellular or nonspecific mitogenic stimuli. *Blood* **99**, 3838-3843 (2002).
214. M. Krampera *et al.*, Bone marrow mesenchymal stem cells inhibit the response of naive and memory antigen-specific T cells to their cognate peptide. *Blood* **101**, 3722-3729 (2003).
215. I. Rasmusson, O. Ringden, B. Sundberg, K. Le Blanc, Mesenchymal stem cells inhibit the formation of cytotoxic T lymphocytes, but not activated cytotoxic T lymphocytes or natural killer cells. *Transplantation* **76**, 1208-1213 (2003).
216. T. V. Johnson *et al.*, Identification of retinal ganglion cell neuroprotection conferred by platelet-derived growth factor through analysis of the mesenchymal stem cell secretome. *Brain* **137**, 503-519 (2014).
217. G. M. Taghi, H. G. K. Maryam, L. Taghi, H. Leili, M. Leyla, Characterization of in vitro cultured bone marrow and adipose tissue-derived mesenchymal stem cells and their ability to express neurotrophic factors. *Cell Biology International* **36**, 1239-1249 (2012).
218. K. Sakai *et al.*, Human dental pulp-derived stem cells promote locomotor recovery after complete transection of the rat spinal cord by multiple neuro-regenerative mechanisms. *Journal of Clinical Investigation* **122**, 80-90 (2012).
219. A. Wilkins *et al.*, Human bone marrow-derived mesenchymal stem cells secrete brain-derived neurotrophic factor which promotes neuronal survival in vitro. *Stem Cell Research* **3**, 63-70 (2009).
220. S. P. Dormady, O. Bashayan, R. Dougherty, X. M. Zhang, R. S. Basch, Immortalized multipotential mesenchymal cells and the hematopoietic microenvironment. *Journal of Hematotherapy and Stem Cell Research* **10**, 125-140 (2001).
221. M. H. Abumaree *et al.*, Human Placental Mesenchymal Stem Cells (pMSCs) Play a Role as Immune Suppressive Cells by Shifting Macrophage Differentiation from Inflammatory M1 to Anti-inflammatory M2 Macrophages. *Stem Cell Reviews and Reports* **9**, 620-641 (2013).
222. A. Ribeiro *et al.*, Mesenchymal stem cells from umbilical cord matrix, adipose tissue and bone marrow exhibit different capability to suppress peripheral blood B, natural killer and T cells. *Stem Cell Research and Therapy* **4**, (2013).

223. R. C. Siqueira, J. C. Voltarelli, A. M. V. Messias, R. Jorge, Possible mechanisms of retinal function recovery with the use of cell therapy with bone marrow-derived stem cells. *Arquivos Brasileiros de Oftalmologia* **73**, 474-479 (2010).
224. Y. O. Joo *et al.*, The anti-inflammatory and anti-angiogenic role of mesenchymal stem cells in corneal wound healing following chemical injury. *Stem Cells* **26**, 1047-1055 (2008).
225. X. X. Jiang *et al.*, Human mesenchymal stem cells inhibit differentiation and function of monocyte-derived dendritic cells. *Blood* **105**, 4120-4126 (2005).
226. W. Zhang *et al.*, Effects of mesenchymal stem cells on differentiation, maturation, and function of human monocyte-derived dendritic cells. *Stem Cells and Development* **13**, 263-271 (2004).
227. M. D. Nicola *et al.*, Human bone marrow stromal cells suppress T-lymphocyte proliferation induced by cellular or nonspecific mitogenic stimuli. *Blood* **99**, 3838-3843 (2002).
228. S. R. Baglio, D. M. Pegtel, N. Baldini, Mesenchymal stem cell secreted vesicles provide novel opportunities in (stem) cell-free therapy. *Front Physiol* **3**, 359 (2012).
229. S. A. Jacobs, V. D. Roobrouck, C. M. Verfaillie, S. W. Van Gool, Immunological characteristics of human mesenchymal stem cells and multipotent adult progenitor cells. *Immunology and Cell Biology* **91**, 32-39 (2013).
230. K. H. Han *et al.*, The immunosuppressive effect of embryonic stem cells and mesenchymal stem cells on both primary and secondary alloimmune responses. *Transplant Immunology* **23**, 141-146 (2010).
231. A. J. Nauta, W. E. Fibbe, Immunomodulatory properties of mesenchymal stromal cells. *Blood* **110**, 3499-3506 (2007).
232. A. Vega *et al.*, Treatment of knee osteoarthritis with allogeneic bone marrow mesenchymal stem cells: A randomized controlled trial. *Transplantation* **99**, 1681-1690 (2015).
233. S. Kern, H. Eichler, J. Stoeve, H. Kluter, K. Bieback, Comparative analysis of mesenchymal stem cells from bone marrow, umbilical cord blood, or adipose tissue. *Stem Cells* **24**, 1294-1301 (2006).
234. Z. Zhou *et al.*, Comparison of mesenchymal stromal cells from human bone marrow and adipose tissue for the treatment of spinal cord injury. *Cytotherapy* **15**, 434-448 (2013).

235. D. Arboleda *et al.*, Transplantation of predifferentiated adipose-derived stromal cells for the treatment of spinal cord injury. *Cell Mol Neurobiol* **31**, 1113-1122 (2011).
236. J. M. Kim *et al.*, Systemic transplantation of human adipose stem cells attenuated cerebral inflammation and degeneration in a hemorrhagic stroke model. *Brain Res* **1183**, 43-50 (2007).
237. K. Sakai *et al.*, Human dental pulp-derived stem cells promote locomotor recovery after complete transection of the rat spinal cord by multiple neuro-regenerative mechanisms. *J Clin Invest* **122**, 80-90 (2012).
238. A. C. M. Assis *et al.*, Time-dependent migration of systemically delivered bone marrow mesenchymal stem cells to the infarcted heart. *Cell Transplantation* **19**, 219-230 (2010).
239. T. V. Johnson *et al.*, Neuroprotective effects of intravitreal mesenchymal stem cell transplantation in experimental glaucoma. *Invest Ophthalmol Vis Sci* **51**, 2051-2059 (2010).
240. A. C. Barber *et al.*, Repair of the degenerate retina by photoreceptor transplantation. *Proceedings of the National Academy of Sciences of the United States of America* **110**, 354-359 (2013).
241. D. Hambright *et al.*, Long-term survival and differentiation of retinal neurons derived from human embryonic stem cell lines in un-immunosuppressed mouse retina. *Molecular Vision* **18**, 920-936 (2012).
242. A. E. Kuriyan *et al.*, Vision Loss after Intravitreal Injection of Autologous "Stem Cells" for AMD. *N Engl J Med* **376**, 1047-1053 (2017).
243. H. Y. Park, J. H. Kim, H. Sun Kim, C. K. Park, Stem cell-based delivery of brain-derived neurotrophic factor gene in the rat retina. *Brain Res* **1469**, 10-23 (2012).
244. P. Whiting, J. Kerby, P. Coffey, L. da Cruz, R. McKernan, Progressing a human embryonic stem-cell-based regenerative medicine therapy towards the clinic. *Philosophical Transactions of the Royal Society B: Biological Sciences* **370**, (2015).
245. B. V. Stanzel *et al.*, Human RPE stem cells grown into polarized RPE monolayers on a polyester matrix are maintained after grafting into rabbit subretinal space. *Stem Cell Reports* **2**, 64-77 (2014).

246. J. Kundu, A. Michaelson, P. Baranov, M. J. Young, R. L. Carrier, in *Developments in Ophthalmology*. (2014), vol. 53, pp. 143-154.
247. I. Tsukahara *et al.*, Early attachment of uncultured retinal pigment epithelium from aged donors onto Bruch's membrane explants. *Experimental Eye Research* **74**, 255-266 (2002).
248. J. C. Booij, D. C. Baas, J. Beisekeeva, T. G. Gorgels, A. A. Bergen, The dynamic nature of Bruch's membrane. *Prog Retin Eye Res* **29**, 1-18 (2010).
249. B. Lu, Y. C. Tai, M. S. Humayun, in *Developments in Ophthalmology*. (2014), vol. 53, pp. 155-166.
250. C. Jiang, H. Klassen, X. Zhang, M. Young, Laser injury promotes migration and integration of retinal progenitor cells into host retina. *Molecular Vision* **16**, 983-990 (2010).
251. M. S. Singh *et al.*, Transplanted photoreceptor precursors transfer proteins to host photoreceptors by a mechanism of cytoplasmic fusion. *Nat Commun* **7**, 13537 (2016).
252. L. Zhou *et al.*, Differentiation of induced pluripotent stem cells of swine into rod photoreceptors and their integration into the retina. *Stem Cells* **29**, 972-980 (2011).
253. E. L. West *et al.*, Pharmacological disruption of the outer limiting membrane leads to increased retinal integration of transplanted photoreceptor precursors. *Experimental Eye Research* **86**, 601-611 (2008).
254. K. Hosoya, M. Tomi, M. Tachikawa, Strategies for therapy of retinal diseases using systemic drug delivery: relevance of transporters at the blood-retinal barrier. *Expert Opin Drug Deliv* **8**, 1571-1587 (2011).
255. M. Takahashi, T. D. Palmer, J. Takahashi, F. H. Gage, Widespread integration and survival of adult-derived neural progenitor cells in the developing optic retina. *Molecular and Cellular Neurosciences* **12**, 340-348 (1998).
256. M. J. Young, J. Ray, S. J. O. Whiteley, H. Klassen, F. H. Gage, Neuronal differentiation and morphological integration of hippocampal progenitor cells transplanted to the retina of immature and mature dystrophic rats. *Molecular and Cellular Neurosciences* **16**, 197-205 (2000).
257. D. M. Chacko, J. A. Rogers, J. E. Turner, I. Ahmad, Survival and differentiation of cultured retinal progenitors transplanted

in the subretinal space of the rat. *Biochemical and Biophysical Research Communications* **268**, 842-846 (2000).
258. S. Singhal *et al.*, Chondroitin sulfate proteoglycans and microglia prevent migration and integration of grafted müller stem cells into degenerating retina. *Stem Cells* **26**, 1074-1082 (2008).
259. I. Sellés-Navarro, B. Ellezam, R. Fajardo, M. Latour, L. McKerracher, Retinal ganglion cell and nonneuronal cell responses to a microcrush lesion of adult rat optic nerve. *Experimental Neurology* **167**, 282-289 (2001).
260. M. Karlstetter, S. Ebert, T. Langmann, Microglia in the healthy and degenerating retina: Insights from novel mouse models. *Immunobiology* **215**, 685-691 (2010).
261. Y. Zhang, H. J. Klassen, B. A. Tucker, M. T. R. Perez, M. J. Young, CNS progenitor cells promote a permissive environment for neurite outgrowth via a matrix metalloproteinase-2-dependent mechanism. *Journal of Neuroscience* **27**, 4499-4506 (2007).
262. L. L. Jones, R. U. Margolis, M. H. Tuszynski, The chondroitin sulfate proteoglycans neurocan, brevican, phosphacan, and versican are differentially regulated following spinal cord injury. *Experimental Neurology* **182**, 399-411 (2003).
263. E. J. Bradbury *et al.*, Chondroitinase ABC promotes functional recovery after spinal cord injury. *Nature* **416**, 636-640 (2002).
264. S. A. Busch, J. Silver, The role of extracellular matrix in CNS regeneration. *Current Opinion in Neurobiology* **17**, 120-127 (2007).
265. J. Silver, J. H. Miller, Regeneration beyond the glial scar. *Nature Reviews Neuroscience* **5**, 146-156 (2004).
266. T. Suzuki *et al.*, Chondroitinase ABC treatment enhances synaptogenesis between transplant and host neurons in model of retinal degeneration. *Cell Transplantation* **16**, 493-503 (2007).
267. A. Zlotnik, O. Yoshie, H. Nomiyama, The chemokine and chemokine receptor superfamilies and their molecular evolution. *Genome Biol* **7**, 243 (2006).
268. A. D. Luster, Chemokines--chemotactic cytokines that mediate inflammation. *N Engl J Med* **338**, 436-445 (1998).
269. Y. Tanaka *et al.*, T-cell adhesion induced by proteoglycan-immobilized cytokine MIP-1 beta. *Nature* **361**, 79-82 (1993).

270. A. Zlotnik, O. Yoshie, The chemokine superfamily revisited. *Immunity* **36**, 705-716 (2012).
271. B. Moser, M. Wolf, A. Walz, P. Loetscher, Chemokines: multiple levels of leukocyte migration control. *Trends Immunol* **25**, 75-84 (2004).
272. H. Nomiyama, N. Osada, O. Yoshie, The evolution of mammalian chemokine genes. *Cytokine Growth Factor Rev* **21**, 253-262 (2010).
273. L. Patel, S. J. Charlton, J. K. Chambers, C. H. Macphee, Expression and functional analysis of chemokine receptors in human peripheral blood leukocyte populations. *Cytokine* **14**, 27-36 (2001).
274. A. Muller *et al.*, Involvement of chemokine receptors in breast cancer metastasis. *Nature* **410**, 50-56 (2001).
275. M. Baggiolini, B. Dewald, B. Moser, Interleukin-8 and related chemotactic cytokines--CXC and CC chemokines. *Adv Immunol* **55**, 97-179 (1994).
276. O. Yoshie, T. Imai, H. Nomiyama, Chemokines in immunity. *Adv Immunol* **78**, 57-110 (2001).
277. D. K. Vassilatis *et al.*, The G protein-coupled receptor repertoires of human and mouse. *Proc Natl Acad Sci U S A* **100**, 4903-4908 (2003).
278. P. J. Lodi *et al.*, High-resolution solution structure of the beta chemokine hMIP-1 beta by multidimensional NMR. *Science* **263**, 1762-1767 (1994).
279. C. Laudanna, J. J. Campbell, E. C. Butcher, Role of Rho in chemoattractant-activated leukocyte adhesion through integrins. *Science* **271**, 981-983 (1996).
280. P. Loetscher *et al.*, The ligands of CXC chemokine receptor 3, I-TAC, Mig, and IP10, are natural antagonists for CCR3. *J Biol Chem* **276**, 2986-2991 (2001).
281. F. Sallusto, A. Lanzavecchia, Understanding dendritic cell and T-lymphocyte traffic through the analysis of chemokine receptor expression. *Immunol Rev* **177**, 134-140 (2000).
282. P. Loetscher, M. Seitz, M. Baggiolini, B. Moser, Interleukin-2 regulates CC chemokine receptor expression and chemotactic responsiveness in T lymphocytes. *J Exp Med* **184**, 569-577 (1996).
283. R. H. Waterston *et al.*, Initial sequencing and comparative analysis of the mouse genome. *Nature* **420**, 520-562 (2002).

284. S. A. Islam *et al.*, Mouse CCL8, a CCR8 agonist, promotes atopic dermatitis by recruiting IL-5+ T(H)2 cells. *Nat Immunol* **12**, 167-177 (2011).
285. V. Alexeev, A. Donahue, J. Uitto, O. Igoucheva, Chemotaxis-driven disease-site targeting of therapeutic adult stem cells in dystrophic epidermolysis bullosa. *Stem Cell Res Ther* **7**, 124 (2016).
286. Z. Shen *et al.*, Genetic modification to induce CXCR2 overexpression in mesenchymal stem cells enhances treatment benefits in radiation-induced oral mucositis. *Cell Death Dis* **9**, 229 (2018).
287. G. Chamberlain, K. Wright, A. Rot, B. Ashton, J. Middleton, Murine mesenchymal stem cells exhibit a restricted repertoire of functional chemokine receptors: comparison with human. *PLoS One* **3**, e2934 (2008).
288. C. Kilkenny *et al.*, Animal research: reporting in vivo experiments--the ARRIVE guidelines. *J Cereb Blood Flow Metab* **31**, 991-993 (2011).